Statistical Beaconing Congestion Control for Vehicular Networks

Esteban Egea-Lopez, Juan J. Alcaraz, Javier Vales-Alonso, *Member, IEEE*, Andreas Festag, *Senior Member, IEEE*, Joan Garcia-Haro, *Member, IEEE*

***Abstract*—Cooperative inter-vehicular applications rely on the periodic exchange of broadcast single-hop status messages among vehicles, called beacons. The aggregated load on the wireless channel due to beacons can prevent the transmission of other types of messages, what is called channel congestion due to beaconing activity. In this paper we propose a novel statistical approach to transmit power control for beaconing congestion control, called Statistical Beaconing Congestion Control (SBCC). Unlike previous proposals, SBCC uses local information, very limited feedback and its implementation is simple. Each vehicle computes locally the power needed to comply with a given maximum beacon load as a function of estimated channel parameters, vehicle density and beaconing rate. A realistic Nakagami-m fading and path loss propagation model is assumed. We provide a final expression of the algorithm as a linear proportional controller, with two variants, SBCC-C and SBCC-N, depending on how the parameters are estimated. Additionally, we derive an expression for the estimated communication range under interference, which approximates the average fraction of packets lost due to hidden node collisions. Finally, we evaluate the performance degradation caused by differences in local vehicle densities and propose a mechanism, called *edge correction*, to limit it while keeping the safety benefits of an extended range at the edge of a cluster of vehicles. SBCC is validated with a realistic hybrid network-traffic simulator and results show that it effectively controls beaconing congestion.**

***Index Terms*—Vehicular Communications, beaconing congestion control, transmit power control (TPC).**

I. Introduction

Inter-vehicle communications based on wireless technologies pave the way for innovative applications in traffic safety, driver-assistance, traffic control and other advanced services which will make up future Intelligent Transportation Systems (ITS) [1]. Communications for Vehicular Ad-Hoc Networks (VANET) have been developed and standardized in the last years. At the moment, a dedicated short range communication (DSRC) bandwidth has been allocated to vehicular communications at 5.9 GHz and both American and European standards [2] have adopted IEEE 802.11p [3] as physical and medium access control layers, based on carrier-sense multiple access with collision avoidance (CSMA/CA). These networks are characterized by a highly dynamic environment where short-life connections between vehicles are expected as well as adverse propagation conditions leading to severe or moderate fading effects [4].

Cooperative inter-vehicular applications usually rely on the broadcast of single-hop status messages among vehicles on a single control channel, which provide detailed information about vehicles position, speed, heading, acceleration and other data of interest [5]. These messages are called *beacons* and are transmitted periodically, at a fixed or variable *beaconing rate*. Beacons provide very rich information about the vehicular environment and so are relatively long messages, between 250 and 800 bytes, even more if security-related overhead is added [5]. In addition, vehicles exchange other messages on the control channel: *service announcements* and *event-driven messages* as a result of certain events. For instance, *emergency* messages are transmitted only when a dangerous situation is detected.

The aggregated load on the wireless channel due to periodic beacons can rise to a point where it can limit or prevent the transmission of other types of messages, what is called *channel congestion due to beaconing activity*. This situation occurs in scenarios with high vehicle density and/or high beaconing rate. To avoid entering the congested channel state there are several options: (1) decreasing the beaconing rate or (2) decreasing the number of vehicles in transmission range of each other or (3) a combination of both of them. The first one is not always appropriate since the quality of service of many applications depends on the beaconing rate, as for instance, the accuracy of the last known position of a given vehicle

E. Egea-Lopez, J. J. Alcaraz, J. Vales-Alonso and J. Garcia-Haro are with the Department of Information and Communications Technologies, Universidad Politecnica de Cartagena (UPCT), Spain, e-mail: esteban.egea@upct.es

A. Festag is with NEC Laboratories Europe and Technical University Dresden, Vodafone Chair Mobile Communications Systems.

This research has been supported by the MINECO/FEDER project grant TEC2010-21405-C02-02/TCM (CALM). It is also developed in the framework of "Programa de Ayudas a Grupos de Excelencia de la Región de Murcia, de la Fundación Séneca, Agencia de Ciencia y Tecnología de la RM".

[6]. Moreover, current standards, e.g. [5], specify a minimum beaconing rate for certain applications. In particular, safety-related applications like "Collision Risk Warning" or "Intersection Collision Warning" require the highest beaconing rate, usually 10 beacons/s. The second solution involves increasing or decreasing the transmit power (*Transmit Power Control, TPC*) to adjust the number of vehicles receiving beacons. But it is still necessary to disseminate vehicle information over a range large enough to support safety applications. Therefore, transmit power must be set at the maximum value possible while keeping the load below a given threshold, called *Maximum Beaconing Load (MBL)*. Finally, the latter option, adjusting both beaconing rate and transmit power, may actually be the only valid approach in certain scenarios, where quality of service and congestion control requirements cannot be met simultaneously. Those cases are usually highly application-dependent [6], [7] and we do not specifically consider them here.

In this paper we focus on the second approach and propose a novel statistical approach to TPC for beaconing congestion control. Since TPC input information and performance is basically driven by stochastic processes, it is natural to take an statistical approach to the design of a TPC algorithm. Controlling instantaneous channel load is neither practical nor useful due to the highly dynamical and broadcast nature of vehicular networks, so we work with average magnitudes. Therefore, we aim at controlling the average beaconing load, which is determined by the average transmission range, density of vehicles and beaconing rate. Indeed, in our proposal, each vehicle computes locally the maximum power needed to comply with a given MBL as a function of the radio channel parameters, vehicle density and beaconing rate. From this approach, we derive an algorithm, called *Statistical Beaconing Congestion Control (SBCC)*, which, as one of our main design goals, can be implemented in real equipment with little effort. Additionally, SBCC has the following features:

- *Based on a realistic channel model*. Radio propagation and fading effects obviously have an important impact on TPC performance since they determine the instantaneous transmission range of a vehicle. To all practical purposes, actual radio signal attenuation is probabilistic in nature due to shadowing and multipath propagation, and so it is more realistically described by probabilistic fading channel models. Hence, we assume a Nakagami-m fading model [8], which can realistically describe a wide range of fading conditions.
- *Local information and limited feedback*. We assume knowledge about channel parameters and vehicle density is not available in advance. Instead, nodes estimate them with simple procedures. As feedback for neighbors, beacons only have to include the transmit power in use, a discrete value [2], which only requires a single additional byte. Except for it, estimation procedures do not add extra overhead to the communications, unlike previous proposals [9].
- *Algorithm simplicity*. We derive two discrete control laws for the transmit power, called SBCC-C and SBCC-N, which are essentially linear proportional controllers [10] and so keep implementation complexity at a minimum. Together with the use of simple estimates, the overall algorithm can be readily implemented in real equipment.

Moreover, we derive an expression for the *estimated communication range under interference*, which is commonly defined, e.g. in standards [11], as "that range where hidden stations do not have a significant impact". It can also be interpreted as the average fraction of packets lost due to hidden node collisions. Hence, it allows to compute metrics such as the effective beaconing rate, which is crucial for many applications. In this proposal we mainly use it to compensate the error in the estimation of the vehicle density in high load conditions. A general problem of TPC schemes is that they may cause asymmetries in transmit ranges between nodes which might result in unacceptable degradation of the performance of some nodes, or local unfairness. We evaluate the degradation caused by differences in local densities and propose a mechanism, called *edge correction* (EC), to limit its impact while keeping the safety benefits of an extended range at the edge of a group of vehicles. The results from this evaluation are also useful to select design parameters, like MBL, for different scenarios. SBCC is validated and evaluated with a realistic hybrid network-traffic simulator and compared with the more relevant previous proposal. Our results show that it is able to effectively control beaconing congestion and improve other performance metrics in dynamic scenarios. Additionally, we show how, as a result of using TPC, the effective beaconing rate is in fact independent of vehicle density and mainly determined by the interference range which only depends on channel parameters, like attenuation and fading.

The remainder of this paper is structured as follows: Section II reviews and discuss recent studies relevant to our work, introducing basic concepts as well. In Section III statistical congestion control is described in several steps: first, the network model as well as the equations that control the average channel load are introduced. Then, parameter estimation procedures are discussed. Afterwards, interference range is derived. Finally, implementation aspects are discussed and the

discrete control laws are derived. In Section IV, asymmetric ranges and performance due to differences in densities are discussed and evaluated, and edge correction is proposed. Section V provides simulation results in a static scenario, used to validate our approach, whereas in Section VI we evaluate the algorithm performance in more realistic dynamic scenarios and compare it with previous proposals. Finally, in Section VII we summarize our contributions and suggest future work.

II. Related Work

We focus on European ETSI standards, though the lower layers are very similar in both American and European specifications. In both of them, IEEE 802.11p provides a CSMA-based medium access control (MAC). Most of the transmissions are broadcast in nature and use a fixed contention window and no acknowledgment or retransmission. ETSI standards specify a 10 MHz control channel for vehicular communications at 5.9 GHz [2]. Periodic beaconing over one-hop broadcast communications supports cooperative inter-vehicular applications by disseminating status and environmental information to vehicles on the control channel, what has been called "Cooperative Awareness Service" [5]. The generation rate of beacons depends on the application and is set by the most demanding one. Since safety-related applications require the maximum beaconing rate of 10 beacons/s [5] it is expected to be the default one. Besides, high vehicle density situations are common [12]. Therefore, straight calculations show that even for moderate transmission ranges, the problem of channel congestion due to beaconing activity has to be taken into account.

Adaptive beaconing rate is a valid solution as long as application quality of service requirements are met, as discussed in [6], [7], [13]–[15]. In both [6], [13] authors evaluate the influence of beaconing rate on the accuracy of the position of neighbors, and in [6] additionally a simple algorithm to adapt transmit power is proposed. Authors of [14], [15] propose transmission rate control algorithms to comply with a generic beacon rate goal, which would be set by an application. Both of them propose linear controls, the former based on continuous feedback whereas the latter on binary feedback. And in both cases transmission range is fixed, according to application requirements, prior to rate adaptation. In this paper, on the contrary, we focus on controlling channel congestion specifically by TPC and in more general scenarios, where vehicles by default keep the channel load under a given MBL unless a particular application triggers a different mechanism. In that case, our proposal can be combined with more specific procedures, as for instance, substituting the fixed values for range and channel parameters in [6] and [15] by our estimates, further improved by taking into account interference as shown in Sect. III-C and Appendix.

TPC, the alternative to adaptive beaconing rate, has been proposed as a mechanism for congestion control by both standards [11] and recent proposals [9], [16]–[18]. A common shortcoming of all these proposals is that they do not consider fading effects on the design of the TPC algorithm. Instead, the influence of a realistic channel is evaluated by simulation. But fading and interference have a relevant effect on the operation of the TPC mechanism because the quality and accuracy of the input information available to the algorithm are actually determined by them: first, ignoring them usually results in an underestimation or overestimation of the transmission range, which degrades the result of the algorithm. Second, vehicles cannot reliably know the real number of neighbors they have in range. That is, since the probability of beacon reception due to fading and packet interference decreases with the distance, vehicles far away are more unlikely to be discovered. When the channel load is high, precisely when TPC is necessary, this problem aggravates. And third, as we will show later in Sect. V, they actually determine the effective beaconing rate received by vehicles and so the quality of the beaconing service itself. Therefore, channel effects and interference should be taken into account directly in the design of algorithms. As an example, OPRAM [19] uses a realistic channel model by design in order to improve the probability of packet reception according to the distance to a potentially dangerous area. The latter is also an example of the related concept of application-based congestion control or awareness control, whose goal is to adapt the power or rate of a subset of nodes in order to comply with some application requirements. A detailed survey of the more relevant application-based as well as congestion control techniques and concepts can be found in [18]. Application requirements are certainly important as discussed in [15], [18] but we focus on a general congestion control procedure first and leave integration of both schemes as future work.

A closely related proposal to ours, since in both cases only power is adjusted in order to comply with a MBL, is D-FPAV [9], a TPC algorithm and protocol to achieve congestion control and fairness. D-FPAV solves a max-min fairness allocation problem in a distributed way. But to do so, nodes have to exchange two-hop neighbor position information piggybacked in *extended beacons*. Hence, the main drawback of D-FPAV is the overhead it adds, which further increases with the number of neighbors. In order to overcome this problem, the authors propose DVDE/SPAV [16], where vehicle

density around every node is estimated and exchanged in a constant-size histogram of the density. Besides, SPAV merges the information of the received histograms from nodes far away to correct the underestimation of the real number of neighbors due to interference. In both cases solving the max-min fairness problem adds complexity to the implementation of the TPC procedure. On the contrary, SBCC requires only to include in beacons the transmit power in use and adds very little complexity to TPC implementation.

Ongoing field trials for vehicular communications have been mainly focused on the assessment of safety and traffic efficiency. Some field trials have also studied channel congestion mitigation techniques. In the United States, the V2V-I project implemented the approaches of [6], and [15] with both binary and continuous feedback. In Europe, the simTD project has tested a TPC algorithm based on a modified version of [16]. The approach proposed in this paper springs from the work in the simTD field trial and attempts to overcome its drawbacks.

Outside vehicular networks, TPC has been substantially applied in cellular networks. A comprehensive recent review can be found in [20]. In [8] it is shown from empirical measurements that a path loss propagation model together with a Nakagami-m fading model describes realistically radio propagation for vehicular networks in different environments. SBCC is based on it, which makes it general enough to be applied under different fading conditions, i.e, different values of m, and enables it to be implemented in real applications. Finally, modeling interference has been extensively studied for years as shown in [21]. Deep and rigorous analysis in the context of poisson processes can be found in [22] and [23], but in most practical cases no closed-form expression is known for the distribution of the aggregated interference. Therefore, to derive the estimated communication range under interference we do not consider the aggregated interference, as is further discussed and justified in Section III and validated later in Section V.

III. Statistical Beaconing Congestion Control

In the following sections we describe our proposal, called Statistical Beaconing Congestion Control for Vehicular Networks (SBCC). First, the system model is introduced and the foundations of our proposal are derived. Afterwards, we discuss the estimation of parameters needed for the procedure. We derive later a formula to compute the interference range or, conversely, the effective range where transmissions are not spoiled by hidden-node collisions. Finally, we propose and discuss a particular implementation of our proposal and derive two simple control laws for transmit power updates.

Notation. From now on random variables are written in boldface letters as $\mathbf{X}$, with probability density function (pdf) $f_{\mathbf{X}}(x)$ and distribution function $F_{\mathbf{X}}(x)$. The following are the most used acronyms and variables.

CBT	Channel Busy Time: fraction of time the channel is detected as busy (received power over sensitivity) by the radio.
ρ	Vehicle density (vehicle/m).
b_s	Beacon size (bits).
b_r	Nominal beaconing rate (beacons/s).
$\bar{b}_r$	Effective beaconing rate: beacons per second correctly received (beacons/s).
MBL	Maximum Beaconing Load: channel load goal. It can be expressed in different ways.
L_M	MBL expressed as bps (bits/s).
C_{max}	MBL expressed as a fraction of the available bandwidth or equivalently as CBT.
N_{max}	MBL expressed as maximum number of vehicles in range given a b_r and b_s (vehicles).
r_{CS}	Average carrier sense range (m).
r_I	Average interference range (m).

A. System model and statistical congestion control

Let us consider a vehicular network on one dimensional manifold and assume a traffic flow with average density of cars ρ vehicles/m. The traffic distribution is not relevant for the problem. Let us assume that vehicles transmit with constant power p over a fading channel with path loss attenuation. For the sake of clarity in the explanation let us assume first that the fading is Rayleigh. Then, the power received at a location y from a transmitter at x is $p\mathbf{F}/l(|x-y|)$, where $l(x)$ is a path loss attenuation model and $\mathbf{F}$ is an exponential random variable with mean 1. We adopt the model proposed by Baccelli [22]: $p\mathbf{F}$ is interpreted as a "virtual power", which is exponentially distributed with mean p, that is, received power becomes $\mathbf{F}/l(|x-y|)$, where transmit power is now an exponential r.v. $\mathbf{F}$, with parameter $\mu = p^{-1}$.

If we consider a more general Nakagami-m model [8] the received power follows a gamma distribution, with parameters m and μ, called *shape* and *scale* parameters respectively. Therefore, the virtual power is a r.v. $\mathbf{F}$, whose pdf is $f_{\mathbf{F}}(x) = \frac{(\mu x)^{m-1}\mu e^{-\mu x}}{\Gamma(m)}$, where $\Gamma(x)$ is the *gamma function*, and parameter $\mu = \frac{m}{p}$ to get an average power of p. The fading intensity is given by the parameter m, a lower value implies more severe fading conditions. Note that when $m = 1$ it is equivalent to Rayleigh fading. We use a one-slope path loss model $l = Ax^{\beta}$, where $A = (\frac{4\pi}{\lambda})^2$, λ is the wavelength of the carrier and β is the *path loss exponent*.

With this model, the probability that the received power at a point at distance y from a transmitter is above the sensitivity

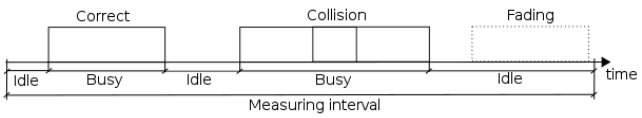

Fig. 1. Channel Busy Time (CBT) measured by a receiver. First packet is correctly decoded. Second and third packets collide with each other. Fourth packet is not detected by the radio due to fading.

of the receiver S, p_{CS}, is :

$$p_{CS}(y) = Pr(\mathbf{F} > SAy^{\beta}) = 1 - F_{\mathbf{F}}(SAy^{\beta}) = \frac{\Gamma(m, \frac{SAy^{\beta}m}{p})}{\Gamma(m)} \quad (1)$$

where $\Gamma(m, x)$ is the *upper incomplete gamma function*.

Therefore, let the transmission range or carrier sense range be the random variable $\mathbf{r}$. Then $Pr(\mathbf{r} > y) = p_{CS}(y)$. And, since $F_{\mathbf{r}}(y) = 0$ for $y < 0$, we can compute its average value r_{CS} as

$$r_{CS} = \int_0^{\infty} \frac{\Gamma(m, \frac{SAy^{\beta}m}{p})}{\Gamma(m)} \mathrm{d}y = \\ = \frac{1}{\Gamma(m)} \int_0^{\infty} \int_{\frac{SAy^{\beta}m}{p}}^{\infty} t^{m-1} e^{-t} \mathrm{d}t \mathrm{d}y \quad (2)$$

Changing the order of integration of the iterated integral we get

$$r_{CS} = \frac{1}{\Gamma(m)} \int_0^{\infty} t^{m-1} e^{-t} \left(\int_0^{(\frac{t}{SA\frac{m}{p}})^{\frac{1}{\beta}}} \mathrm{d}y \right) \mathrm{d}t = \\ = \frac{1}{\Gamma(m)} \int_0^{\infty} t^{m-1} e^{-t} \left(\frac{t}{SA\frac{m}{p}} \right)^{\frac{1}{\beta}} \mathrm{d}t = \frac{\Gamma(m + \frac{1}{\beta})}{\Gamma(m)(SA\frac{m}{p})^{\frac{1}{\beta}}} \quad (3)$$

Let us note that we use indistinctly transmission range and carrier sense range as that one where the signal from a transmitter can be detected. However, for a packet to be correctly decoded, the SINR has to be greater than a certain value T, which results in a smaller *effective* transmission range. Nevertheless, from the point of view of congestion control both cases are equivalent: the channel is considered busy and so it is not available for transmission. In fact, although MBL is usually expressed as a percentage of the channel data rate, an alternative metric is *Channel Busy Time* (CBT) defined as the fraction of time that a receiver considers the channel occupied in a time interval, as exemplified in Fig. 1. CBT is commonly measured by standard network hardware and can be made available by the driver software. However, this is an aggregated metric, that is, from the measured CBT the contributions of different classes of traffic cannot be distinguished.

Then, assuming all vehicles use the same power, the average channel load is given by:

$$L = 2 r_{CS} \rho b_r b_s \quad (4)$$

where b_r is the average beaconing rate in hertz or beacons/s, b_s the average beacon size in bits, and L is expressed in bps.

From eq. (3) and (4), any vehicle can compute the maximum power p^* to be used in order to keep the average load under a given MBL, L_M:

$$p^* = SAm \left(\frac{L_M \Gamma(m)}{2\rho b_r b_s \Gamma(m + \frac{1}{\beta})} \right)^{\beta} \quad (5)$$

Therefore, our proposal to control congestion is to make every vehicle compute and set the maximum power p^* that keeps load under the goal MBL, L_M, according to vehicle density ρ and to channel conditions, summarized by the path loss exponent β and shape parameter m. These values are not known *a priori* and change over time, so vehicles have to periodically estimate them from the information they have available. In the following sections we propose estimates for them. Congestion control is applied in a distributed way: channel load generated by surrounding neighbors is measured, either using vehicle density or CBT as discussed in Sect. III-D, and transmit power is increased or decreased according to eq. (5) and using the estimated channel parameters. In an ideal scenario, all the neighbor vehicles act in the same way, collectively raising or lowering the channel load. But since vehicles in a realistic deployment do not use exactly the same power, we propose to use an average of the neighboring powers, which becomes an additional feedback for the control. In practice, therefore, vehicles do not exactly measure the same environmental conditions in all the cases. The implications of this fact are discussed and evaluated in Sect. IV.

Before going on let us introduce the following remarks to clarify matters and assumptions:

- Transmission range and vehicle density are independent random variables and so the average load is given by the multiplication of their average values.
- Beaconing rate is not actually independent of the other variables. That is, we can distinguish three rates: nominal beaconing rate, b_r, transmitted beaconing rate, b'_r, and effective beaconing rate, $\bar{b}_r$. The first one is the beaconing offered load, whereas b'_r is the rate actually transmitted by the vehicle after MAC operation, which contributes to channel load. At high load conditions the MAC saturates and beacons are discarded. Thus, b'_r in fact depends on the vehicle density. However, we assume that TPC is able to reduce the number of neighbors before the MAC enters saturation. Therefore, we consider $b_r \approx b'_r$ and independent of vehicle density and transmit power. On the other hand, effective beaconing rate, $\bar{b}_r$, is the rate of beacons correctly received from a neighbor. Once

TPC is working, it is determined by fading and hidden node collisions, as shown in Fig. 1. The fraction of packets lost due to fading is accounted for with the average carrier sense radius, r_{CS} and so b_r is the correct rate to appear in eq. (4). To account for the losses due to hidden-node collisions we compute the estimated communication range under interference in Sect. III-C. These assumptions are validated and further discussed in Sect. V.

- A vehicle will consider the channel busy either if it can decode packets or they are corrupted by hidden-node collisions or interference, as depicted in Fig. 1. However, since part of the interfered transmissions overlap, measured CBT is lower than the corresponding to load given by eq. (4). For congestion control it is acceptable since the channel load overestimation results in lower transmit power p^*, that is, a worst case approach. Again, the estimated communication range under interference can be used to approximate the fraction of packets lost by hidden-node collisions and correct the value of L.
- In the remainder of the paper we will consider constant beacon size b_s and nominal beaconing rate b_r. Setting b_r to its highest value, 10 beacons/s, as demanded by safety-related applications, would reduce the information needed to be collected and result in a worst case approach.

Finally, let us remark that transmit power is not expected to converge to a single value for every vehicle. It would be possible in an ideal case, with perfect knowledge and continuous transmit power. But, in real vehicles, power can only take discrete values, and the algorithm is based on estimates of the parameters, so vehicles compute different values of the transmit power. Indeed, transmit power is expected to vary over an average value as the environment estimates are updated. For that same reason SBCC cannot *guarantee* that load is strictly below a MBL. On the contrary, load is expected to oscillate around the goal MBL value, which should be assigned a safety margin. We come back to this matter in Sect. III-D and IV.

B. Estimation of channel parameters

Channel conditions are reflected on the path loss exponent β and m parameter. Vehicles can estimate their value from the information carried by beacons collected from other vehicles and their own low-level measurements. Let us note here that path loss estimation has been extensively studied and many approaches are available, as discussed in [24]. In addition, since it is a large scale and slow-varying parameter [8], it may not be necessary its estimation in a real deployment. We describe next a simple dynamic estimation for the sake of example and evaluation, in case no suitable method were available. We assume a single slope model and vehicles collect a sample of it from every beacon as $\beta_i = ln(\frac{P_{t,i}}{AP_{r,i}})/ln(\Delta_x)$, where ln is the natural logarithm, $P_{t,i}$ and $P_{r,i}$ are respectively the transmit and received power for the packet, and Δ_x is the distance between transmitter and receiver. $P_{t,i}$ and the vehicle position are carried by beacons, whereas $P_{r,i}$ can be provided by common network hardware. In real hardware, though, the reported received power includes energy from interfering signals and so alternative methods may be necessary [24]. The estimate for the path loss exponent $\hat{\beta}$ is simply the sample mean of the last N_β collected samples, or a moving average of them to reduce potential oscillations.

To estimate m, we would need samples of the virtual power $\mathbf{F}$, which is gamma distributed, and so it will differ from the real transmit power reported in beacons. Thus, vehicles collect samples of the virtual power F_i from the received power as $F_i = AP_{r,i}(\Delta_x)^{\hat{\beta}}$. Accurate estimation of the shape parameter of a Nakagami-m model has been the subject of several works [25]. However, we do not actually need extreme accuracy in our proposal. In fact, to account for the effect of interference, as discussed next in Sect. III-C, we assume an Erlang distribution and approximate m by its nearest integer. Therefore, to estimate m we can use the method of [26], which is simpler and provides a better estimation for small sample sizes, resulting in $\hat{m} = \frac{(\bar{F})^2}{S^2} - \frac{1}{N_m}$, where $\bar{F}$ and S^2 are the sample mean and sample variance respectively over a sample of size N_m. Anyway, the main problem is that all methods require i.i.d. samples [25]. Whereas samples are indeed independent, they are not identically distributed, because vehicles use different transmit powers. But, since transmit power is discrete in practice, vehicles can keep a set of samples for every power step. This way, separated sets of samples for every step are collected to compute $\hat{m}$ after collecting N_m samples of a particular step. In Section V we validate the estimates and show that they provide reasonably accurate values.

C. Estimated communication range under interference

The estimated communication range under interference is commonly defined, e.g. in standards [11], as "that range where hidden stations do not have a significant impact". Being able to estimate this range allows to determine the effective transmission range of packets (not only beacons) and so the effective beaconing rate received by the vehicles, which may be lower than the nominal one due to hidden node collisions.

To compute the estimated communication range we derive

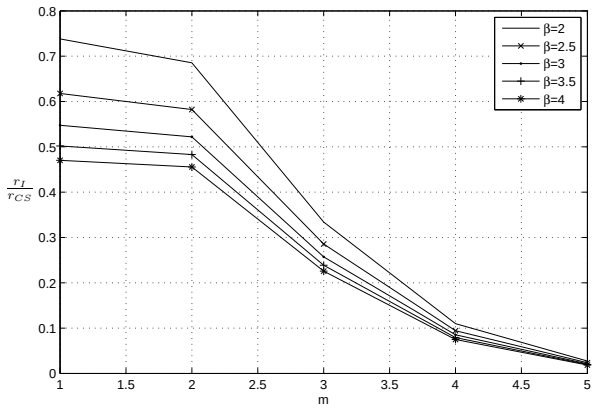

Fig. 2. Normalized interference range: fraction of transmission range corrupted by interference due to hidden nodes versus m parameter and path loss exponent, assuming equal transmit power for transmitter and interferer.

first what we call the interference range for the assumed Nakagami-m model. Since there is no common definition for this range, let us clarify that we here refer to the average fraction of the average transmission range where packets are corrupted by hidden node interference. To simplify the derivation of the interference range, r_I, we bring up the following assumptions:

- First, correct packet reception depends on the SINR being greater than a given threshold T. We assume that noise is negligible compared to interference. And we only consider the power of a single interferer (hidden node). This assumption is reasonable since (1) the contention-based MAC layer (802.11p) successfully prevents simultaneous transmissions within r_{CS}, so hidden nodes must be outside this range and (2) the network is one-dimensional, so any other simultaneously transmitting node must be located at least r_{CS} m away from the hidden node which makes the aggregated interference low enough to be negligible.
- Second, we consider a saturated situation, where all the stations always have a packet to transmit, which is a good approximation under high load conditions.

As shown in Appendix, the interference range is given by

$$r_I = r_{CS}\frac{\mu_T^m}{(m-1)!}\sum_{i=0}^{m-1}\frac{1}{i!}\left[\int_1^\infty \frac{(\frac{\mu_H}{T}(\alpha-1)^\beta)^i}{(\mu_T+\frac{\mu_H}{T}(\alpha-1)^\beta)^{m+i}}\cdot \right.$$
$$\left.\cdot\frac{(m+\frac{1}{\beta})_i}{(1+\frac{\mu_H}{T\mu_T}(\alpha-1)^\beta)^{\frac{1}{\beta}}}\frac{\alpha-1}{\alpha}\mathrm{d}\alpha\right] \quad (6)$$

where $\mu_T = {p_T}^{-1}$ and $\mu_H = {p_H}^{-1}$ are the inverse of the power of transmitter and hidden node (interferer) respectively. The integral of eq. (6) has to be solved numerically. It can be done in real time by vehicles. Otherwise, their values can be tabulated and stored.

Let us note that it can be expressed as the fraction of the transmission range where packets are corrupted by hidden node interference, that is, define the normalized interference range $\bar{r}_I = \frac{r_I}{r_{CS}}$. Thus, the average *estimated communication range under interference* is $r_E = r_{CS} - r_I = r_{CS}(1-\bar{r}_I)$. Figure 2 shows the normalized interference range. As can be seen, the interference range for severe fading conditions and low attenuation can be remarkably high. The interpretation of this range is twofold. On the one hand, it can be seen as the average fraction of transmission range where vehicle transmissions are not reliable. On the other hand, it shows the average fraction of packets lost because of interference. That is, sometimes even packets from close neighbors are also lost due to hidden node collisions because of fading. For instance, according to this latter interpretation, for $\beta = 2.5$ and $m = 1$ and very high channel load conditions, a vehicle is expected to lose up to 60% of all the transmitted beacons, as results shown in Sect. V confirm.

SBCC in particular uses the interference range for what we call *interference correction* technique to correctly estimate the surrounding vehicle density under high load conditions. Vehicles can estimate the vehicle density by the position information collected from neighbor beacons in different manners. In low channel load conditions, a simple estimate is to just divide the average number of neighbors discovered, $\hat{N}$, by the average transmission range r_{CS}, that is, $\hat{\rho} = \frac{\hat{N}}{2r_{CS}}$.

However, r_{CS} only accounts for packets lost because of fading but in high channel load conditions hidden node collisions also corrupt beacon reception. We can use the interference range to correct the density estimation in those cases. In particular, it is more effective when used together with the measured CBT, as follows. Looking at Fig. 1, a busy interval due to hidden node collisions can be approximated to last 1.5 times the duration of a beacon on the average and involves at least two beacons from neighbors. Then the average fraction of time occupied by interfered transmissions is approximately $t_I \approx 2\rho r_{CS} 1.5 b_t \bar{r}_I b_r/2$, where b_t is the duration of a beacon. Whereas the average fraction of time occupied by correct transmissions is $t_C \approx 2\rho r_{CS} b_t(1-\bar{r}_I)b_r$. Since measured CBT is $\hat{c} = t_C + t_I$, we get then the estimated density as:

$$\hat{\rho} = \frac{\hat{c}V_t}{2b_r b_s r_{CS}(1-0.25\bar{r}_I))} \quad (7)$$

where V_t is the transmission bitrate in bps and $\hat{c}$ is CBT measured over a period of time. Therefore, hidden node collisions make measured CBT be lower than that provided by eq. (4) by a fraction of approximately $1-0.25\bar{r}_I$. Let us

note here that it results in a "compression factor", dependent on the fading but independent of traffic density and power used, which agrees with previous results [27].

Similarly, used with $\hat{N}$ the estimate becomes:

$$\hat{\rho} = \frac{\hat{N}}{2r_{CS}(1-\bar{r}_I))} \tag{8}$$

In this case, the estimate is rougher because over a measurement period not all the beacons from a given neighbor are lost due to interference. In Sect. III-D we discuss when to use this correction mechanism.

D. Implementation as discrete controls

The foundations of our proposal have been laid in previous sections. However, to develop a practical implementation there are still a number of matters to decide and refine. In this section we propose a particular implementation and discuss related matters. Other implementations and additional refinements are possible.

As main result from this section we derive two alternative control laws for transmit power based on how the vehicle density is measured: neighbor-based (SBBC-N) or CBT-based (SBCC-C) controls. The reason for these two variants is that estimating the number of neighbors in range is prone to a number of issues, some of them depending on the implementation. Thus, an alternative is to directly measure CBT, though it also has limitations. The major design decisions are discussed in the next paragraphs and then the controls are derived and discussed.

- *Congestion Control triggering*. We propose that vehicles periodically adapt their transmit power on the basis of the estimated environment parameters. That is, vehicles collect samples of reception power, transmit power and location from received beacons and keep a table of known vehicles. After a given sampling period, T_s, they compute the maximum power to comply with the MBL, according to channel and load estimates from collected samples, and apply it. Current vehicle hardware provides measurements of received packet power but only allows to set transmit power in discrete steps. Standards specify that it shall be set in 0.5 dB steps [2]. Therefore, vehicles set the transmit power to the largest step available below p^*. Due to the logarithmic scale of transmit power setting, discretization error is smaller at low powers, which benefits congestion control. In any case, vehicles will always use the maximum power possible as long as it complies with the MBL, which is the intended goal.
- *Number of neighbors and CBT*. Accurate knowledge of the number of neighbors a vehicle has is difficult even in absence of interference. Vehicles usually keep a *neighbor table* with information collected from beacons, which is updated every time a new beacon is received. To account for neighbors leaving, outdated information is deleted after a *table update time*, which makes the perceived number of neighbors depend on the update time. If its value is high, vehicles overestimate the number of neighbors. An alternative estimate is given by the measured CBT $\hat{c}$, which can be provided by networking hardware as specified in [5]. Using CBT to estimate the number of neighbors has also limitations: It is an aggregated metric, so when other kind of traffic is present it should be disaggregated.
- *Interference correction*. Either if neighbor table or CBT is used, we use the proposed interference correction mechanism. Interference correction is only used under high load conditions. That is, when measured CBT is above a certain threshold I_T, interference correction is triggered and vehicle density is computed according to eq. (7) or eq. (8). When CBT falls below the threshold, interference correction is deactivated. It also provides a fast recovery mechanism: if the load rises above the threshold it triggers a quicker reduction of transmit power.
- *Average neighbor transmit power*. Neighbor vehicles do not use the same power due to differences in parameter estimation and load measurements. Instead of computing r_{CS} assuming equal power, every vehicle computes its neighboring "average" carrier sense range as $\hat{r}_{CS} = \frac{1}{N}\sum_i^N r_{CS,i} = M\sum_i^N p_i^{\frac{1}{\beta}}/N = M\bar{p}_n$. That is, vehicles compute a sample mean of the carrier sense range according to the transmit power in use included in beacons from neighbors, where M is just the part of eq. (3) not dependent on p. $\bar{p}_n$ is computed as a moving average to reduce oscillations. The average transmit power of neighbors is important for the controls we derive next, since it acts as one of the main feedback inputs.

With all the previous mechanisms in place, we can provide a final expression for the control law used for transmit power. Depending on how the vehicle density is estimated there are two variants.

Neighbor-based control (SBBC-N). When the neighbor table is used, we insert into eq. (5) the expression for the estimate of density in eq. (8) and transmission range in eq. (3), to get

$$p^* = \left(\bar{p}_n \frac{(1-\bar{r}_I)L_M}{\hat{N}b_r b_s}\right)^{\hat{\beta}} = \left(\bar{p}_n \frac{(1-\bar{r}_I)N_{max}}{\hat{N}}\right)^{\hat{\beta}} \tag{9}$$

where $\bar{p}_n$ is computed from neighbor transmit powers as discussed above. The ratio of MBL to beaconing rate and beacon size gives the maximum number of neighbors in range

to keep that load, so it has been called N_{max}. Since estimates are computed periodically every T_s s, transmit power can be expressed as a discrete control:

$$p^*[n+1] = \left\lfloor \left(\bar{p}_n[n](1-\hat{r}_I[n]) \frac{N_{max}}{\hat{N}[n]} \right)^{\hat{\beta}[n]} \right\rfloor \quad (10)$$

where, $\bar{p}_n[n]$, $\hat{N}[n]$ and $\hat{\beta}[n]$ are computed from samples collected over the previous T_s s. Additionally, $\hat{m}[n]$ is computed from samples in order to obtain $\hat{r}_I[n] = \bar{r}_I(\hat{m}[n])$.

CBT-based control (SBCC-C). Similarly, when measured CBT is used to estimate the vehicle density, the control we get is:

$$p^*[n+1] = \left\lfloor \left(\bar{p}_n[n](1-0.25\hat{r}_I[n]) \frac{C_{max}}{\hat{c}[n]} \right)^{\hat{\beta}[n]} \right\rfloor \quad (11)$$

where C_{max} is MBL expressed as a fraction of data rate and $\hat{c}[n]$ is the measured CBT over the previous T_s s.

In both cases, $\lfloor x \rfloor$ means that the power selected is the highest power step no greater than x and interference correction is only applied when the load is above a given threshold, otherwise $\hat{r}_I[n] = \bar{r}_I(\hat{m}) = 0$.

Both controls should be equivalent, but in practice they are not because of different reasons discussed later in Sect. V. SBCC-C effectively controls the measured load in terms of CBT, whereas SBCC-N actually controls the number of neighbors measured.

Finally, in logarithmic scale both controls have the form $p^*[n+1] = K_n[n] + K_p[n]e[n]$. That is, both controls use as local error signal $e[n]$ the difference between the maximum load value and the measured value, either expressed as neighbors or CBT. So these controls are essentially linear proportional controllers [10], but with a non-tunable proportional gain K_p given by the path loss exponent estimate. There is an additional neighbor feedback input $K_n[n]$, provided by the transmit power used by neighbors, whose role is discussed next.

IV. Differences in densities and edge correction

A general problem of TPC schemes is that they may cause asymmetries in transmit ranges between nodes which might result in degradation of the performance of some nodes, or local unfairness. These asymmetries are mainly caused by differences in either the local vehicle density or its perception by the nodes. In this section we further discuss features and behavior of the proposed SBCC controls, evaluate the degradation caused by such non-homogeneous densities and propose a mechanism to overcome it while keeping the benefits of asymmetric transmit power regarding traffic safety. The results from the evaluation are also useful to appropriately select design parameters, like MBL, for different scenarios.

A. Some remarks on SBCC controls features and behavior

Regarding the information needed to implement the controls, let us first remark that:

- Traffic density is not finally present in the equations, since it is expressed in terms of measured CBT or neighbors in eq. (7) and (8). Hence, it is not necessary to explicitly compute the estimated density unless it is necessary for other purposes.
- The m parameter only needs to be estimated for interference correction actually. The reason is that the measured load and neighbors, $\hat{c}$ and $\hat{N}$, implicitly reflect the actual channel path loss and fading conditions. Looking at eq. (7) and (8), if we fix the real density ρ, the measured load and neighbors depend on the average carrier sense radius r_{CS}, which in its turn, is a direct result of the actual channel conditions.

Regarding the behavior, let us highlight the following remarks:

- *R1*. The controls basically adjust, via transmit power, the average carrier sense range linearly in order to keep an average number of neighbors in range. That is, given a traffic density ρ, controls try to keep the load at C_{max} or, equivalently, at N_{max}, so that $2r_{CS}\rho = N_{max}$.
- *R2*. As long as the average number of nodes in range is lower than N_{max} the power will keep at the maximum.
- *R3*. When the number of nodes is higher than that limit, the power selected is p^*, which results in a new r^*_{CS} such that $2r^*_{CS}\rho = N_{max}$.
- *R4*. Both SBCC controls as given by equations (10) and (11) are driven by two different inputs: a local measurement of the channel load, given by $\hat{c}$ or $\hat{N}$, which reflect both the underlying traffic density and channel conditions; and the feedback collected from neighbor vehicles in the form of the transmit power used, and summarized in $\bar{p}_n$. The former mainly controls the load when nodes use similar powers. The latter reacts to strong asymmetries in power and limits unfairness situations.
- *R5*. A typical unfairness problem of TPC occurs when two clusters of nodes use different transmit power, as depicted in Fig. 3. If controls were driven just by local load measurements, nodes on the left which receive an extra load, could only decrease their power, even to the point of stopping transmission. However, with SBCC that reduction is compensated with the increase in $\bar{p}_n$, caused by the higher powers used from the nodes on the right. The higher the difference of power used, the higher the

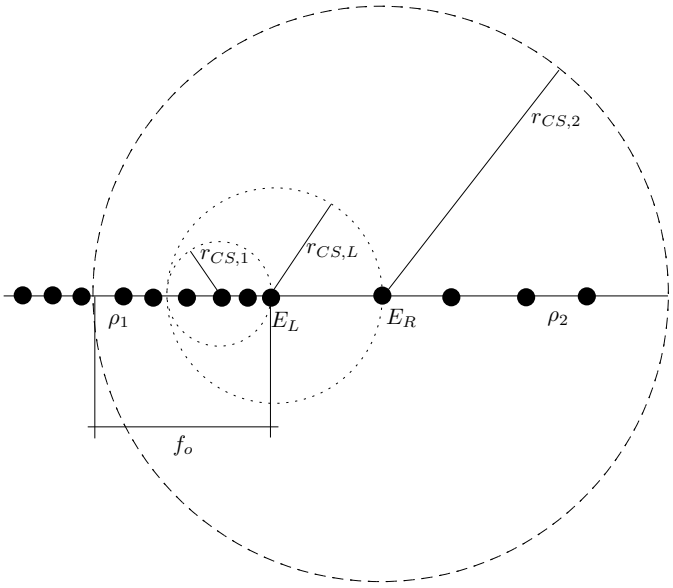

Fig. 3. Differences in local densities result in asymmetric transmission ranges. Two clusters of nodes with densities ρ_1 and ρ_2 respectively.

increase in the collected $\bar{p}_n$. It results in an increase in transmit range from the left side, which consequently forces a power reduction on the other side because of both the increase in load and a lower neighbor average power $\bar{p}_n$ computed on the right side.

The above remarks describe qualitatively the behavior of the controls. We leave as future work a more detailed analysis of the dynamics and stability of the controls. At the moment, we focus on their behavior with respect to strong and sustained differences in local densities. In that case, transmit power asymmetries may persist when, from remarks *R3* and *R4* above, both clusters have previously settled on powers such that dynamics described in *R5* are not enough to re-balance the situation.

Such high differences of density may occur in various situations, for instance, when vehicles approach a traffic jam, although they should be mainly transient. In the following section the degradation of performance in those cases is evaluated.

B. Extra load due to differences in local densities

In this section we estimate the performance degradation due to different local densities in the worst case, that is, when one of the cluster of nodes is as close as possible but not in range of the other, depicted in Fig 3. This is a first approximation, since we are using average values for ranges. In a real scenario, fading effects make some of the packets of each cluster reach each other, which contribute to balance power as described in *R5* above.

Let us assume two different traffic densities $\rho_1 > \rho_2$, which makes nodes select power $p_1 < p_2$, respectively, in order to have $r_{CS,1} = N_{max}/2\rho_1$ and $r_{CS,2} = N_{max}/2\rho_2$, according to *R3* above. In this case, a fraction of the nodes on the left are receiving extra load from nodes on the right, which are not aware of them. Moreover, this extra load makes the total load be above the goal C_{max}; otherwise nodes on the left would be transmitting at maximum power according to *R2* above.

Let us evaluate this extra load in the worst case, considering average values for carrier sense range and load and uniform densities. The fraction of length f_o receiving extra load and the amount of load depends on the distance between the two clusters, and it is maximum when the distance between the edge nodes in the clusters E_L and E_R is equal to $r_{CS,L}$, being $f_o = r_{CS,2} - r_{CS,L}$, see Fig. 3. Here we are considering that the edge node E_L is using a transmit power $p_e > p_1$, since it has been measuring a lower load. In fact, since its local vehicle density is roughly equal to $\rho_1/2$, it is using the power necessary to have $r_{CS,l} = N_{max}/\rho_1$. This same reasoning would apply to E_R, which would be using a higher power than p_2, but in order to consider the worst case, let us assume that it is already the maximum one, that is, $p_2 = p_{max}$. Therefore, the length bearing an extra load is $f_o = r_{CS,2} - r_{CS,L} = \frac{N_{max}}{2}(\frac{1}{\rho_2} - \frac{2}{\rho_1})$. Every node in f_o is receiving an extra amount of load $l_e = f_o \rho_2 \frac{b_r b_s}{V_t}$, from nodes on the right cluster. This extra load is proportional to its position within f_o, being maximum for the edge node E_L.

Nodes close to the edge bear a lower ordinary load than the ones in the center of the cluster, and the extra load can be roughly compensated by the reduced one. However, as we move away from the edge node, the extra load on the nodes decreases proportionally to the distance, but the ordinary one increases. As a consequence, the load is maximum at the closest point to the edge where nodes receive the maximum ordinary load plus the extra one, which is at $1.82 r_{CS,1}$ from E_L, as shown in next subsection. At this point the extra load from the right cluster is:

$$\begin{aligned} l_{em} &= (r_{CS,2} - 3.82 r_{CS,1}) \rho_2 \frac{b_r b_s}{V_t} = \\ &= (r_{CS,2} - 3.82 r_{CS,1}) \frac{N_{max}}{2} \frac{b_r b_s}{V_t} = \\ &= \frac{C_{max}}{2} (1 - \frac{3.82 \rho_2}{\rho_1}) \end{aligned} \tag{12}$$

So, the extra load received depends on the ratio of densities but is not greater than $C_{max}/2$. The maximum occurs there as long as the ratio of densities makes the extra load positive. Indeed, there are constraints on the densities that have to be taken into account. The discussed worst case holds for $2\rho_2 \leq \rho_1$. The maximum density of ρ_1 is physically limited

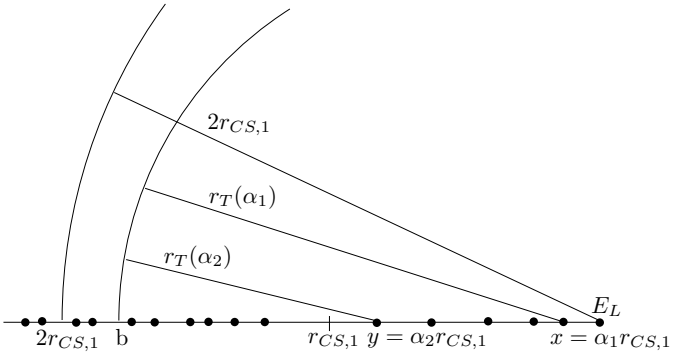

Fig. 4. Example of different average transmission ranges r_{CS} for edge nodes.

by the capacity of the road. A value of $\rho_1 = 0.1$ veh/m can be considered high and corresponding to a congested high-capacity road [12]. On the other hand, the maximum power in use is also limited by the density. That is, if we assume as a worst case that $p_2 = p_{max}$, then $\rho_2 < N_{max}/2r_{CS,max}$, because of *R2* above. So, the longer the effective range in use, the lower the density, which limits the number of vehicles contributing an extra load. Moreover, eq. (12) is independent of the channel conditions, since the controls take care of adapting the power to the fading conditions. The above reasoning is confirmed by our results in Sect. V and VI. Strong differences in local density should not be common. Even though, the performance estimates in this section allows to select the MBL value, C_{max}, with an appropriate safety margin to limit the degradation.

C. Edge correction

From the discussion in the previous subsections, it is clear that *nodes at the edge of a cluster will use a higher power* than those on the center because their local density is lower, which we call an *edge effect*. From a safety perspective, this is a positive feature of SBCC controls, since *it provides an extended warning range for vehicles approaching the cluster*. It is in fact the desired behavior in a traffic jam, for instance.

However, from the point of view of congestion control, the extended range of edge nodes results in an extra load of nodes at a certain distance from the edge. In the worst case, when a strong difference of density between separated clusters is present, as in the scenario of previous subsection, this extra load would add to that of eq. (12). Therefore, we would like to apply a mechanism that would mitigate the negative effects of the extra load while keeping the safety benefits of an extended warning range at the edge. In this section we derive the extra load due to the extended range and afterwards propose such a mechanism.

Let us consider an isolated cluster of nodes with density ρ_1. As before, since SBCC adapts the average transmission range linearly to the surrounding density, the edge node E_L is using a power p_e which results in $r_{CS,L} = 2r_{CS,1}$ because its local density is $\rho_1/2$. Similarly, a node located at a position $x = \alpha r_{CS,1}$, expressed as a fraction of the average carrier sense range, would use a power that results in a range proportional to its local density or equivalently to the load, which is $C_{max}/2$ from its left side and $\alpha C_{max}/2$ from its right side. Hence, the resulting total average range is $r_T(\alpha) = r_{CS,1}\alpha + 2r_{CS,1}/(1+\alpha)$.

Now, given a point b on the left of $r_{CS,1}$ the equation $r_T(\alpha)/r_{CS,1} = b = 1 + 2/(1+\alpha)$ is quadratic and has two solutions $\frac{1}{2}(b - 1 \pm \sqrt{-7 + 2b + b^2})$, denoted α_1 and α_2 respectively, resulting in the same total range. An example is illustrated in Fig. 4. A minimum occurs at $\alpha_m = 0.41$ giving $r_T(\alpha_m) = 1.82 r_{CS,1}$. At that point, the extra load due to the edge nodes is maximum. Therefore, for a point b corresponding to a pair of solutions α_1 and α_2 , the extra load is that corresponding to the fraction of nodes up to α_1 plus the fraction of nodes from α_2 up to $r_{CS,1}$ minus the ordinary load corresponding to those nodes, that is:

$$l_{ed}(b) = (\alpha_1 + b - 1 - \alpha_2)\frac{C_{max}}{2} = 2\alpha_1 \frac{C_{max}}{2} \qquad (13)$$

As we said, this extra load is not desirable, but we would like to let a fraction of nodes on the edge (from E_L to $r_{CS,1}$) transmit at a higher power, dictated by SBCC controls, to keep an extended safety range. Our proposal is to add an *edge correction factor*, K_e, to the controls to force part of the nodes on the edge to transmit at a reduced power and let a fraction α_s to keep the higher power, providing the extended range. This way the fraction of nodes from α_s up to $r_{CS,1}$ would reduce its power as follows. First, the extra range depends on the position of the node $r_e = 2r_{CS,1}/(1+\alpha)$. To avoid further disruptions of the normal operation of the controls for the rest of nodes we keep this range equal to $r_{CS,1}$, so that $r_e K_e = r_{CS,1}$ and $K_e = \frac{1+\alpha}{2}$. Second, nodes have to determine its position on the edge, that is, its own α. From the position information of the beacons, nodes can classify them according to those coming from vehicles ahead or behind, in two fractions f_a and f_b, respectively. Those fractions differ noticeably for nodes on the edge, proportionally to α, as $f = \alpha/(1+\alpha)$, with $f = \min(f_a, f_b)$.

To summarize, to apply *edge correction*, nodes:

1) At each sampling period, classify beacons into two fractions f_a and f_b, according to the position of the source.
2) Given a safety fraction α_s and a margin fraction α_m,

nodes compute K_e from $f = \min(f_a, f_b)$ as

$$K_e = \begin{cases} \frac{1}{2}(1 + \frac{f}{1-f}) & \text{if } \frac{\alpha_s}{1+\alpha_s} < f < \frac{\alpha_m}{1+\alpha_m} \\ 1 & \text{otherwise} \end{cases} \quad (14)$$

3) Nodes set the next power multiplying eq. (11) or (10) by $K_e^{\frac{1}{\beta}}$.

This way, the excess load due to edge effects is kept at $\alpha_s \frac{C_{max}}{2}$. The margin fraction α_m is used to take into account that in reality the fraction of beacons from ahead and behind is not exactly symmetric. Edge correction works better for SBCC-C since it acts directly on the measured load and avoids neighbor table bias. Anyway, this simple mechanism can be refined in a number of ways in a real implementation, and the values for α_s and α_m may be set dynamically.

V. Validation

In this section we test the validity of assumptions and estimates. For the validation we simulate a static scenario, where vehicles do not move and so we can set up an homogeneous vehicle density.

Validation confirms our assumptions which are next summarized before discussing them in detail.

- Not using TPC results in unacceptable degradation of performance in all the cases.
- SBCC-C effectively keeps the measured CBT at the goal C_{max}, whereas SBCC-N keeps the measured number of neighbors at N_{max}. Therefore, both of them achieve their goal although it is not equivalent in terms of channel load.
- When TPC is used, the effective beaconing rate becomes on the average independent of vehicle density and determined essentially by channel parameters, like attenuation and fading. Therefore, they should be taken into account when designing beaconing rate control algorithms.
- Interference range, r_I, provides a close estimate of the fraction of packets lost due to hidden node collisions. It can be used to compute the effective beaconing rate and the actual CBT generated.
- When SBCC is used, average channel access time is around a few ms and beacons are not discarded, which confirms that MAC does not enter saturation.
- SBCC achieves results similar to SPAV [16] with low protocol overhead and algorithm complexity.
- Edge correction effectively reduces the extra load due to edge effects while preserving the extended safety range for nodes on the edge of a cluster.
- Our estimates provide good approximations to system parameters.

TABLE I
Parameters for Static Scenarios (Validation)

Scenario	Parameters
1: low density, severe fading.	$\beta = 2.2$ $m = 1$ $\rho = 0.07$
2: low density, moderate fading.	$\beta = 2.2$ $m = 3$ $\rho = 0.07$
3: high density, severe fading.	$\beta = 2.2$ $m = 1$ $\rho = 0.25$
4: high density, moderate fading.	$\beta = 2.2$ $m = 3$ $\rho = 0.25$
5: high density, severe fading, higher path loss.	$\beta = 2.5$ $m = 1$ $\rho = 0.25$
6: high density, moderate fading, higher path loss.	$\beta = 2.5$ $m = 3$ $\rho = 0.25$

TABLE II
Common Parameters for Simulations

Parameter	Value
Data rate (V_t)	3 Mbps
Sensitivity (S)	-95 dBm
Frequency	5.9 GHz
Maximum Power	1000 mW
Minimum Power	0.1 mW
Power step	0.5 dB
Noise	-110 dBm
SNIR threshold (T)	4 dB
Neighbor Table update time	1 s
Sample period T_s	0.5 s
Beacon size (b_s)	500 bytes
Beaconing rate (b_r)	10 beacons/s
Interference correction threshold (I_T)	0.85

Validation setup. The simulations have been done with OMNET++ and its inetmanet extension [28], which implements the 802.11p standard. This library also implements a realistic reception and interference model, where all the interfering (simultaneously being transmitted) signals plus the noise are added and SINR is evaluated to determine correct packet reception. In addition, capture effect is also implemented.

Vehicles are located on a straight single lane road according to a Poisson point distribution of average density ρ vehicles/m, which is constant during the simulation. We have evaluated both a extremely high vehicle density scenario and a more common situation, with $\rho = 0.25$ and $\rho = 0.07$ vehicles/m respectively. The total length of the road length has been set to obtain an average of 400 vehicles for each simulation. We first remove edge effects, and results are only averaged for the 200 central vehicles. Path loss exponent has been set to $\beta = 2.2$ and $\beta = 2.5$. Values reported by [8] are slightly higher but they have been measured in suburban scenarios. Higher values result in shorter transmission range and so congestion is more unlikely and its effects milder. Thus, those values model a worst case scenario. Nakagami-m shape parameter has been set to $m = 1$ and $m = 3$, to model severe (Rayleigh) and moderate fading conditions respectively. Values reported by [8] suggest even stronger fading. The Maximum Beacon Load has been set to $L_M = 2.1$ Mbps, which is 70% of the available data rate of 3 Mbps, and can be expressed as

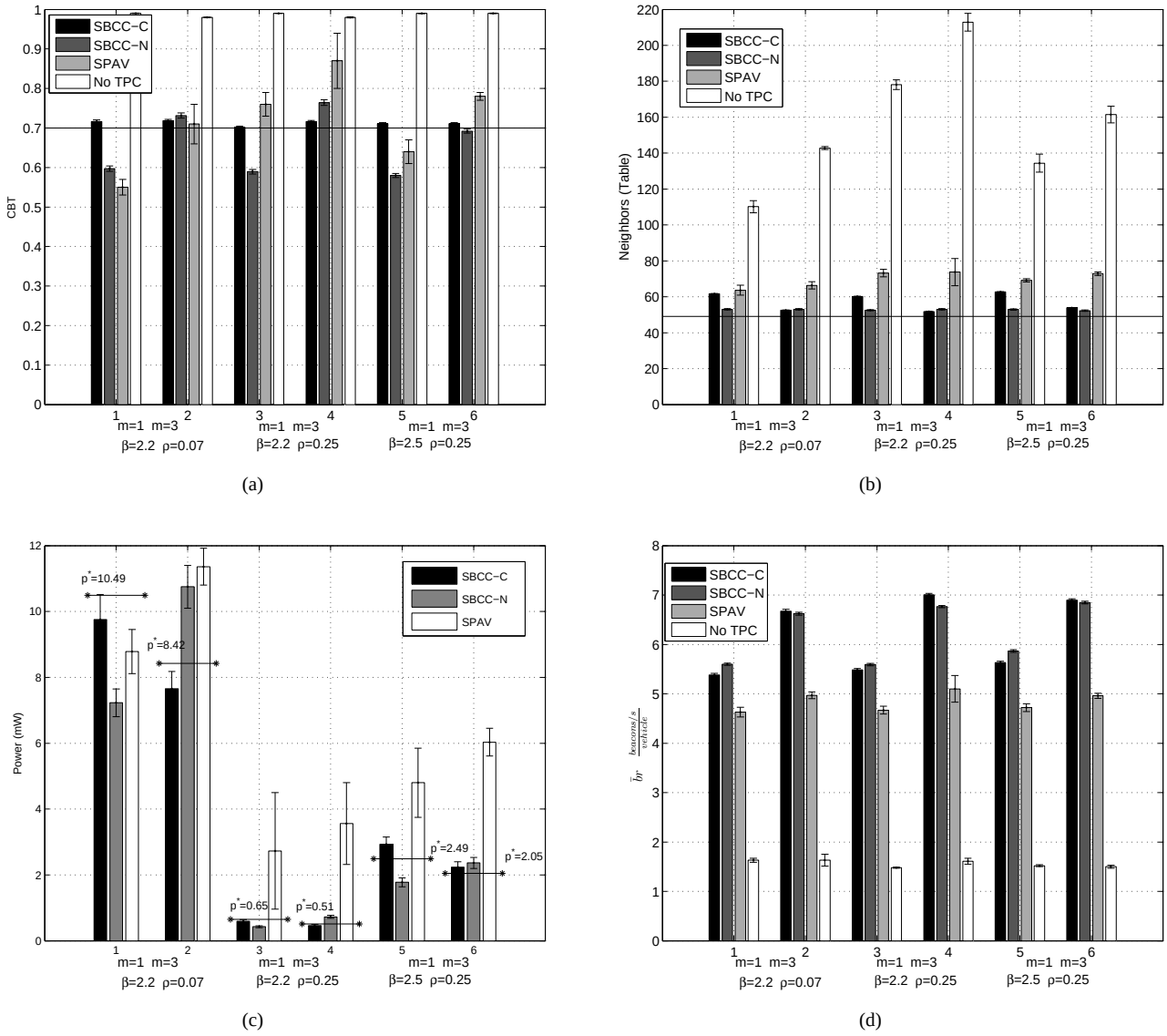

Fig. 5. Performance results for static scenarios (Validation). (a) Average Channel Busy Time (CBT). MBL goal $C_{max} = 0.7$ shown as solid line. (b) Average number of neighbors in neighbor table, $\hat{N}$. MBL goal $N_{max} = 49.15$ shown as solid line. (c) Average power used (mW). Solid lines show p^* and its value for each scenario. For No TPC vehicles use 1000 mW all the time. (d) Average effective beaconing rate per neighbor, $\bar{b}_r$ beacons/s/vehicle.

CBT, $C_{max} = 0.7$, or neighbors, $N_{max} = 49.15$. Scenario-specific parameters are shown in Table I, whereas Table II summarizes the rest of common parameters. Let us note that this combination of data rate and beacon size results in a frame duration that can be over the coherence time of the channel. We assume it is below but close as a worst-case approach. Simulations run for 25 s with 4 s of transient period and have been replicated 15 times with different seeds.

Performance results are shown in Figure 5, with its 95% confidence interval, depicting time-averaged channel busy time, time-averaged number of neighbors in neighbor table, time-averaged power used and average effective beaconing rate per neighbor. Shown confidence intervals have been computed over the averages of replications. The confidence intervals over all the nodes of a single replication are of the same order than the global ones and not shown. We compare not using TPC at all with the two controls discussed in this paper, CBT-based (SBCC-C) and neighbor-based (SBCC-N), as well as SPAV, the algorithm proposed in [16]. It has been selected because it is the more relevant proposal which only adjusts transmit power to control congestion.

Congestion control. Regarding congestion control, results show that both controls fulfill their job, which is in fact different as we said previously: SBCC-C effectively controls the measured CBT, whereas SBCC-N actually controls the measured number of neighbors. Therefore, as expected SBCC-

C keeps the measured CBT at the goal level, $C_{max} = 0.7$, whereas SBCC-N keeps the average number of neighbors in the neighbor table at the goal level of $N_{max} = 49.15$, as can be seen in Fig. 5(a) and Fig. 5(b) respectively. But with SBCC-N the measured CBT may deviate up to 10% above and below the goal. Apparently, controlling the measured CBT should be equivalent to control the number of neighbors. However, it is not the case because of interference mainly. In Fig. 5(c) we show the goal powers p^* for each scenario according to eq. (5), which does not take into account interference. Hence, measured CBT, $\hat{c}$, used as error signal by SBCC-C in eq. (11), is lower than expected by eq. (4) due to time-overlap of hidden node collisions, as depicted in Fig. 1. To compensate for it and keep the load at the desired level, SBCC-C instead correctly selects a slightly higher power in the high-density cases, as we can see in Fig. 5(c) too. On the other hand, SBCC-N uses as error signal the number of known neighbors. Looking at Fig. 5(c), it depends again on fading conditions: severe fading makes SBCC-N select powers lower than the goal, because far away vehicles have a chance to be discovered. Conversely for moderate fading. In this case, the effect of interference takes over. In any case, the difference in average power accounts for the measured CBT, as discussed later in this section.

Effective beaconing rate and interference. Beaconing congestion control main goals are ensuring channel availability for different kinds of traffics and improving the reliability of beacon reception. Fig. 5(d) shows the effective beaconing rate, $\bar{b}_r$, that is, average number of beacons per second correctly received per neighbor. Use of congestion control effectively improves this metric compared to not using TPC. However, it is not possible to achieve the nominal beaconing rate, $b_r = 10$ beacons/s. In fact, for a given attenuation (β) the effective beaconing rate is determined basically by fading conditions and hidden node collisions (interference). We can see that TPC makes the average effective beaconing rate: (1) independent of the vehicle density, (2) almost equal for equal shape parameter m and (3) slightly higher for higher β. The reason is clear: given a vehicle density, TPC fulfills its goal and adjusts the communication range to cover a maximum number of neighbors, N_{max}. Then, correct beacon reception depends on channel conditions and hidden collisions, which, in their turn, depend mainly on fading intensity. Let us remark that the beacon *reception probability* still depends on the actual distance to the source, the transmit power and the channel conditions as given by eq. (1). In short, with TPC nearby vehicles still have a better reception probability and higher powers result in higher probability receptions at longer distances. For instance, at r_{CS} the probability of reception is between 0.46 and 0.51. In particular, for scenario 1 and 2 is 0.46 in both cases, whereas r_{CS} reaches 98 m and 351 m respectively. TPC basically scales the power to keep roughly equal reception probabilities at *equivalent* distances for different local densities.

Computation of effective beaconing rate and CBT with $\bar{r}_I$. Our proposal for congestion control can be basically seen as a method to adjust the power in a way that the number of neighbors in our average communication range is not greater than a given $N_{max} = 2\rho r_{CS}$. Since packet losses due to fading are averaged in r_{CS}, a vehicle should receive correctly b_r beacons from N_{max} neighbors in a sampling period, *but only in absence of interference*. Otherwise, the average fraction of packets lost due to interference is given by the normalized interference range $\bar{r}_I$. Therefore, the average effective beaconing rate should approximately be $N_{max} b_r (1 - \bar{r}_I) \approx \bar{b}_r \hat{N}'$. Here, to avoid the table update bias of $\hat{N}$, we introduce[1] $\hat{N}'$ which is the number of distinct neighbors discovered every T_s s. Now, the effects of hidden node collisions are shown by comparing the above equation with the results. We find that: (1) $\bar{b}_r < b_r$, which indicates that a fraction of beacons from some of the neighbors are lost as expected; and (2) $\hat{N}' < N_{max}$, which shows that *all* the beacons of some neighbors are lost and vehicles are not aware of them. As an example, for Scenario 1 and SBCC-C we have that $\hat{N} = 44.61$ and $\bar{b}_r / b_r = 0.519$ so $39.72 \cdot 0.51/49.15 = 0.47$ which is approximated by $1 - \bar{r}_I$, see Fig. 2, though better than expected. The reason is that $\bar{r}_I$ is computed assuming that hidden node collisions occur always, which is only reasonable in very high channel load conditions. In any case, the main conclusion to draw is that beaconing rate control algorithms, such as [6], [7] should also take into account by design channel conditions and interference as well as the intended application.

Similarly, the CBT caused by a number of neighbors or vehicle density can be quantified correctly using interference range. Results validate that measured CBT can be approximated by $\hat{c} = 2\rho r_{CS}(1 - 0.25\bar{r}_I) b_r b_s / V_t$. One has to be careful to use the carrier sense given by the actual power used. For instance, in scenario 2, SBCC-N averaged power used is 10.75 mW, which results in $r_{CS} = 392.32$ m, giving $\hat{c} = 0.72$ which is in good agreement with results in Fig. 5(a).

Channel access and other proposals. Applying congestion control additionally improves other performance metrics such as average channel access time. Although not shown here, our results for average channel access time are quite similar for all TPC proposals, around 3 ms, and are well below the

[1]Results for $\hat{N}'$ have been collected although they are not shown due to lack of space.

50 ms of timing requirements specified in standards [5]. We have also checked that the MAC does not enter saturation and beacons are never discarded, which confirms that $b'_r = b_r$. From another point of view, overall results show how severe fading conditions have a negative impact on packet probability reception and hidden node collisions, and so the effective beaconing rate is lower for these scenarios. But, on the other hand, fading tends to benefit congestion control since it reduces the aggregated interference and so power can be kept at a slightly higher level. In other words, for a given power level moderate fading improves packet reception probability and so the effective beaconing rate but the measured CBT is higher. Interestingly our results are similar to those of SPAV [16], a low-overhead version of D-FPAV [9] which solves a max-min fairness problem to achieve congestion control. That is, our proposals achieve a similar goal with very limited feedback and without the additional algorithm complexity introduced by SPAV and overhead of D-FPAV. Assuming transmit power is sent with an additional byte, SBCC overhead is 0.21% whereas that of D-FPAV is between 16.2 to 41.4 % and SPAV is 0.42% [16]. Finally, if no power control is applied performance degrades to unacceptable levels. CBT at 0.9 shows that the channel is collapsed due to transmissions and collisions and so vehicles cannot transmit beacons in due time. Average access time is above 0.5 s and more than 80% of the beacons are lost.

Edge correction and difference of densities. In Fig. 6 we show validation results for the scenarios discussed in Sect. IV. First, we have simulated the worst-case scenario for a static difference of densities. Vehicles on the left are positioned uniformly with a density $\rho_2 = 0.02$ which is the maximum density needed to have a maximum transmit power with $\beta = 2.5$ and $m = 3$. Vehicles on the right are positioned starting 200 m away from the edge node on the left, with density $\rho_1 = 0.126$ corresponding to a congested traffic situation. This way, the distance between clusters corresponds to the worst-case situation where the extra load is maximum. As can be seen in Fig. 6(a), edge nodes on the right cluster bear an extra load roughly corresponding to that of eq. (12) which occurs around $2r_{CS,1}$, as discussed in Sect. IV-B. This extra load due to the left cluster adds to the one corresponding to edge effects. It does not reach the expected maximum precisely because the SBCC-C tries to compensate it on both sides, as can be seen from the reduction of load on the edge of the left cluster. Applying edge correction with $\alpha_s = 0.1$ reduces the edge effect contribution to the extra load as expected: 0.035 of excess load for each cluster. The safety goal is also achieved, since 10% of the leftmost edge nodes on the right cluster use a power that results in an average range of 435 m, compared to the average range of 185 m on the center of the cluster. Further reduction of the load in such a extreme situation would require to lower the global MBL threshold or additional mechanisms. In Fig. 6(b) we plot results for scenario 4 with and without edge correction again. This is the more demanding scenario for load control, but edge correction is able to keep the extra load at 0.035 as intended, being maximum again around $2r_{CS,1} = 198$ m, with the extended safety range equal to 271 m on the average. Finally, Fig. 6(c) and 6(d) compare the results with edge correction for all the scenarios, now taking into account also the edges, i.e., all the 400 vehicles, in the averages. As can be seen, the reduction of load in the edges contribute to a global reduction of the average load.

Algorithm	$\hat{\rho}$	$\hat{\beta}$	$\hat{m}$
Scenario 1. $\beta = 2.2$ $m = 1$ $\rho = 0.07$			
SBCC-C	0.07 ± 0.002	2.24 ± 0.005	1.50 ± 0.03
SBCC-N	0.07 ± 0.004	2.24 ± 0.004	1.47 ± 0.024
Scenario 2. $\beta = 2.2$ $m = 3$ $\rho = 0.07$			
SBCC-C	0.07 ± 0.003	2.22 ± 0.001	3.68 ± 0.007
SBCC-N	0.06 ± 0.007	2.22 ± 0.001	3.60 ± 0.042
Scenario 3. $\beta = 2.2$ $m = 1$ $\rho = 0.25$			
SBCC-C	0.27 ± 0.012	2.26 ± 0.007	1.47 ± 0.040
SBCC-N	0.27 ± 0.016	2.26 ± 0.007	1.44 ± 0.027
Scenario 4. $\beta = 2.2$ $m = 3$ $\rho = 0.25$			
SBCC-C	0.26 ± 0.012	2.22 ± 0.002	3.64 ± 0.027
SBCC-N	0.22 ± 0.021	2.22 ± 0.002	4.59 ± 0.042
Scenario 5. $\beta = 2.5$ $m = 1$ $\rho = 0.25$			
SBCC-C	0.26 ± 0.010	2.58 ± 0.007	1.37 ± 0.033
SBCC-N	0.28 ± 0.012	2.57 ± 0.007	1.36 ± 0.034
Scenario 6. $\beta = 2.5$ $m = 3$ $\rho = 0.25$			
SBCC-C	0.25 ± 0.011	2.53 ± 0.002	3.53 ± 0.035
SBCC-N	0.24 ± 0.019	2.53 ± 0.002	3.47 ± 0.039

TABLE III
ESTIMATES FOR STATIC SCENARIOS (VALIDATION)

In summary, in both cases we confirm that edge correction achieves its goal as well as the validity of the estimates for the extra load provided in Sect. IV. Even though they are approximations, they can be used to set values for design parameters such as the MBL.

Estimates. In order to validate our assumptions we also provide results for estimates in Table III, where the average values for $\hat{\rho}$, $\hat{\beta}$, $\hat{m}$ are shown. As can be seen, the path loss exponent β is correctly estimated in all the cases. The shape parameter m is generally overestimated, though vehicles take the nearest integer, which becomes correct for low values, but still is overestimated for high values.

The estimated vehicle density $\hat{\rho}$, measured by the vehicles, is also shown for validation purposes, though it is not directly used by the controls. It has been estimated with eq. (7) and

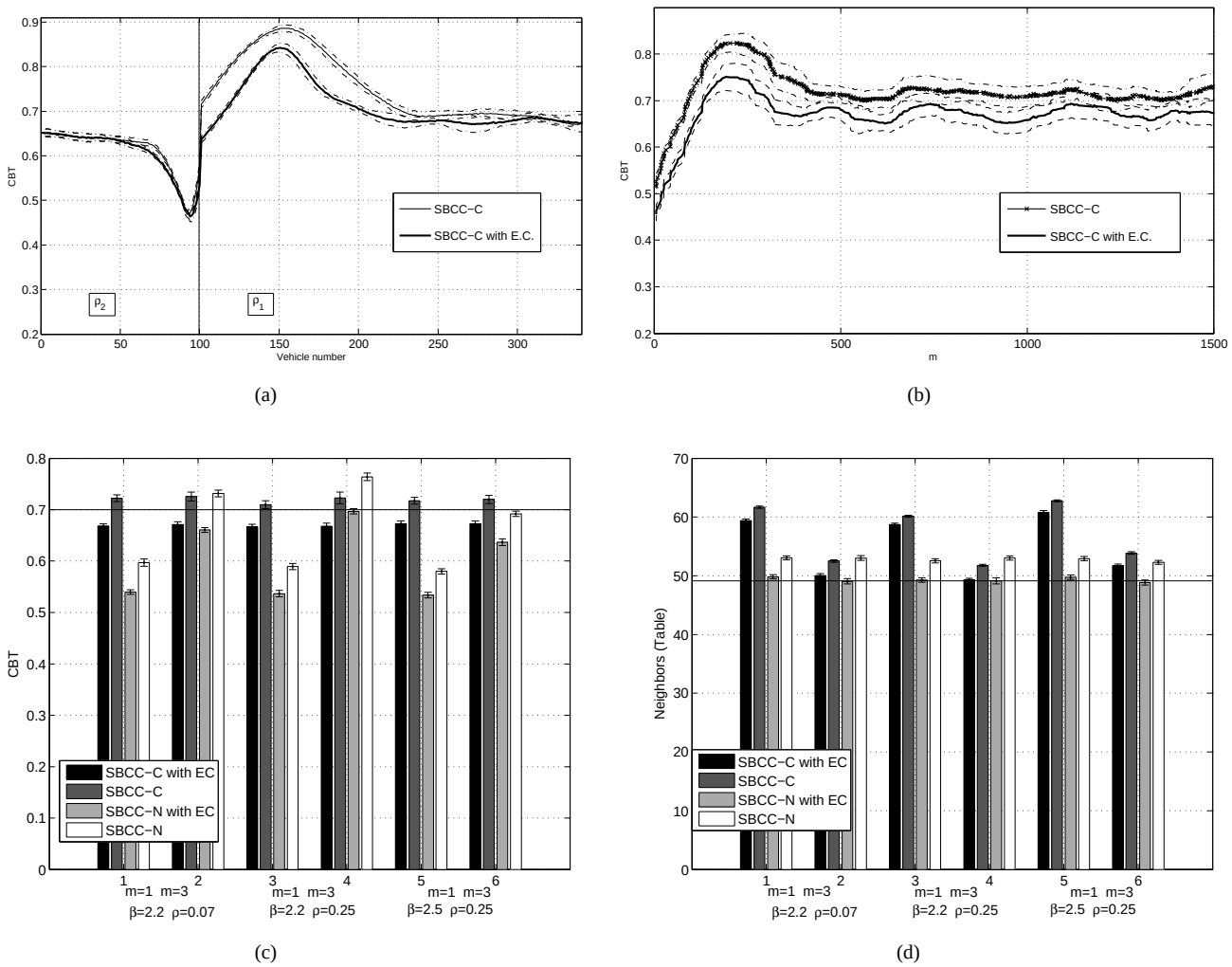

Fig. 6. Performance results for static scenarios with and without *edge correction* (EC), $\alpha_s = 0.1$ and $\alpha_m = 0.8$. (a) Average Channel Busy Time (CBT) for densities $\rho_1 = 0.126$ and $\rho_2 = 0.02$. To avoid the difference of scale in meters due to different densities, X axis shows vehicle numbers equally spaced. Density ρ_2 ends at node 100. (b) Average Channel Busy Time (CBT) for scenario 4 versus vehicle position at the road. (c) Average Channel Busy Time (CBT). MBL goal $C_{max} = 0.7$ shown as solid line. (d) Average number of neighbors in neighbor table, $\hat{N}$. MBL goal $N_{max} = 49.15$ shown as solid line. In (a) and (b), 95% confidence intervals of 15 replications are shown as dashed lines, whereas in (c) and (d) as error bars.

(8) for SBCC-C and SBCC-N, respectively. Average vehicle density is correctly estimated in general, though results tend to be slightly overestimated and better for SBCC-C. Interference correction has been applied when the load is above 0.85, which occurs rarely, and so its influence in the estimation in these tests falls within the confidence interval.

VI. Results

In this section we evaluate and compare our proposals in realistic dynamic scenarios. In this case, the traffic density is not homogeneous anymore and local densities differ over time and at several locations on the road. Moreover, we simulate a traffic jam in order to test SBCC with and without *edge correction* in presence of strong differences of local densities. To this purpose we have run simulations with Veins [29], a hybrid network-traffic simulator which uses OMNET++ [28] as network simulator and SUMO [30] as traffic simulator. We have imported a segment of the A5 German highway from OpenStreetMap [31] between the exits of Kronau and Bruchsal, which goes straight from north to southwest. This is a high-capacity three-lane per direction highway. We have set up flows for two different traffic situations. The first one (Scenarios 1 and 2) models normal traffic conditions, with a flow of cars in both directions driving at high speed with a 5% of heavy and slow vehicles, like trucks. SUMO reports an average flow of 1100 vehicles per lane per hour and an average speed of 32 m/s. The second one (Scenarios 3 and 4) models a traffic jam. The flows are the same but the speed for a segment of the road in the south direction has been artificially limited to 3.33 m/s which makes car slow down and create a traffic jam. Scenarios 1 and 2 have been simulated

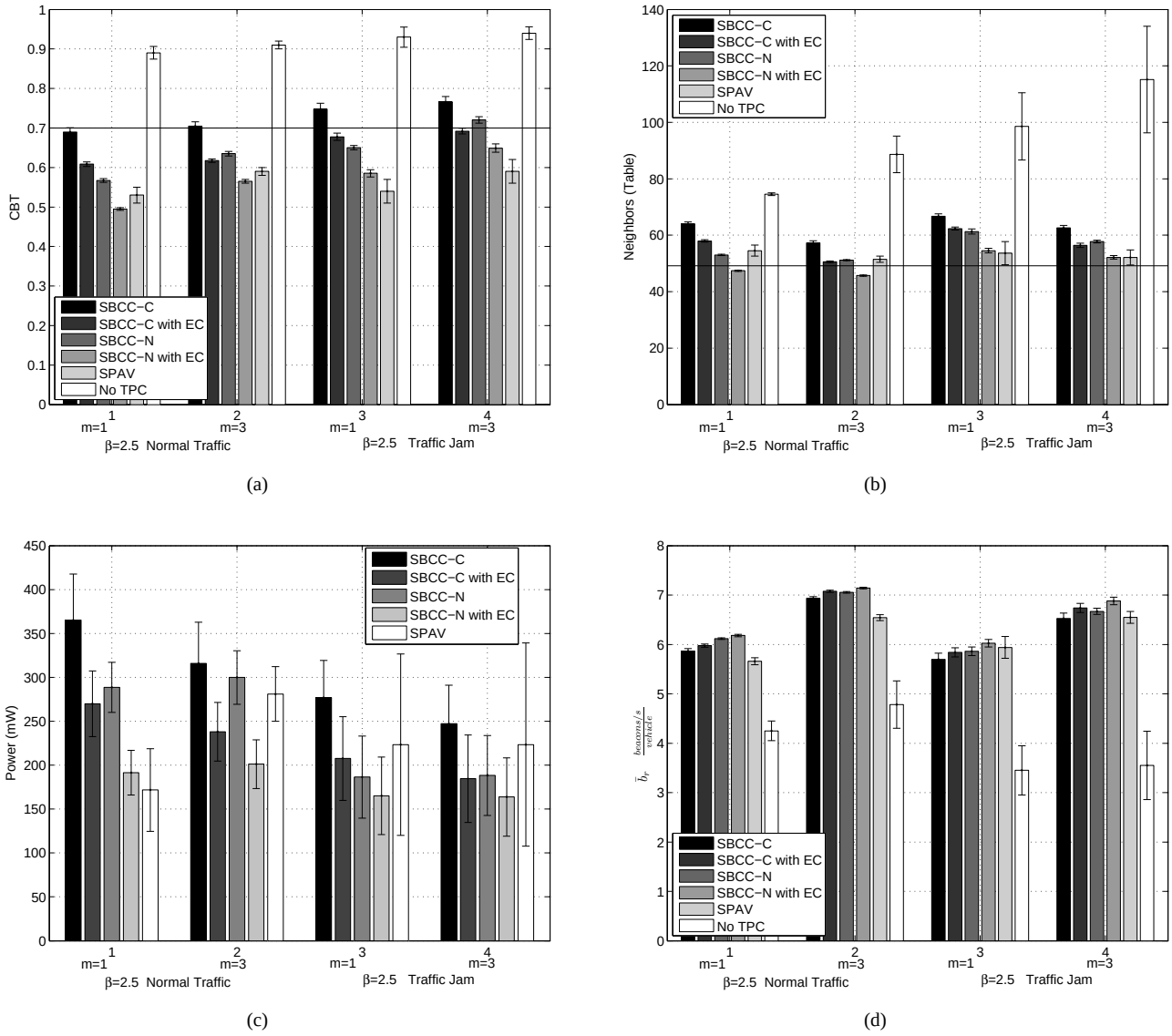

Fig. 7. Performance results for dynamic scenarios: A5 highway with moderate traffic and traffic jam. (a) Average Channel Busy Time (CBT). MBL goal $C_{max} = 0.7$ shown as solid line. (b) Average number of neighbors in neighbor table. MBL goal $N_{max} = 49.15$ shown as solid line. (c) Average power used. For No TPC vehicles use 1000 mW all the time. (d) Average effective beaconing rate per neighbor, $\bar{b}_r$.

for 1000 s, covering a 3.8 Km segment, whereas scenarios 3 and 4 have been simulated for 600 s, covering a 3 Km segment. Each vehicle spends an average of 115 s within the simulation area in the first case and 280 s in the second case. Finally, we have simulated both traffic simulations for severe, $m = 1$ and moderate $m = 3$ fading conditions, with a path loss exponent of $\beta = 2.5$. Each simulation has been replicated 10 times. Again, we set up MBL to 70% of the available bandwidth, or equivalently $C_{max} = 0.7$ and $N_{max} = 49.15$. Fig. 7 shows results for the performance metrics described in the previous Section with 95% confidence intervals. Similarly, Table V shows results for estimates.

Scenario	Parameters
1: A5 highway with normal traffic.	$\beta = 2.5 \quad m = 1$
2: A5 highway with normal traffic.	$\beta = 2.5 \quad m = 3$
3: A5 highway with traffic jam.	$\beta = 2.5 \quad m = 1$
4: A5 highway with traffic jam.	$\beta = 2.5 \quad m = 3$

TABLE IV
PARAMETERS FOR DYNAMIC SCENARIOS

Regarding congestion control, results for CBT in Fig. 7(a) clearly confirm that our proposals work properly also for dynamic scenarios. In all the scenarios the channel load is kept at the desired level. SBCC-N tends to be more conservative in dynamic scenarios because the number of known neighbors keeps higher. The reason is that vehicles detect far away

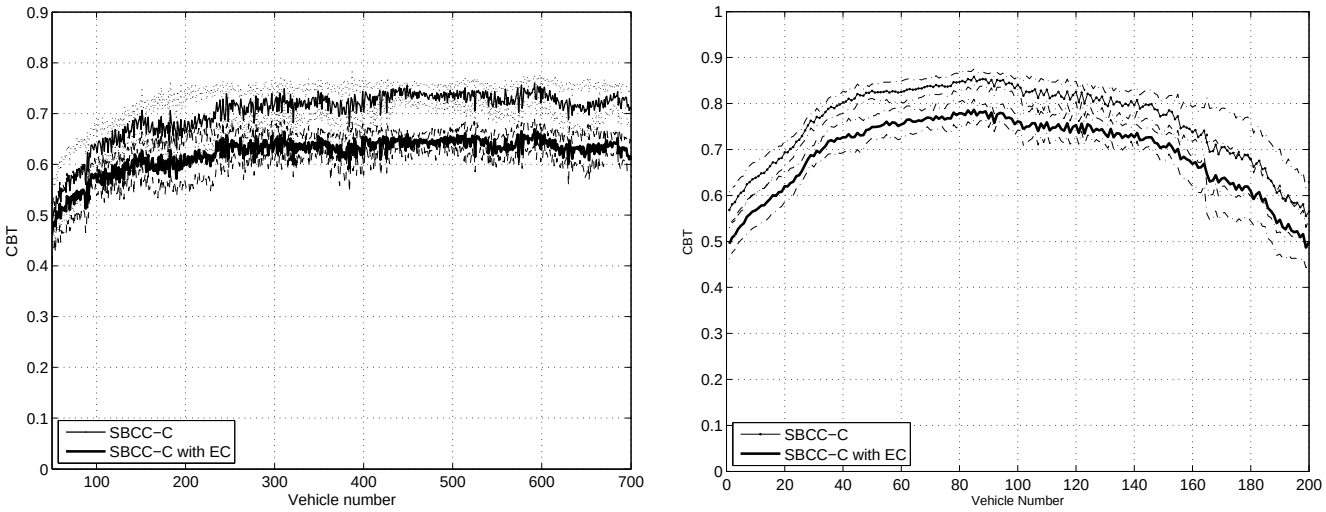

(a) (b)

Fig. 8. Average CBT per vehicle for Scenarios 1 and 3 for SBCC-C with and without *edge correction* (EC), with $\alpha_s = 0.15$ and $\alpha_m = 0.8$. The x-axis shows the vehicle number which is assigned monotonically as each vehicle is created in the simulation. (a) Average CBT per vehicle in A5 with Normal Traffic, $\beta = 2.5$ and $m = 1$. (b) Average CBT per vehicle in A5 with Traffic Jam, $\beta = 2.5$ and $m = 1$. Dash and dotted lines show 95% confidence intervals for 10 replications.

neighbors that use high power until they adjust it according to the environment. More specifically, the simulation operation makes new vehicles appear at one end of the segment and disappear at the opposite end. These new vehicles start using the maximum power and then gradually reduce their power. Therefore, SBCC-N tries harder to reduce the power in order to decrease the number of neighbors in range. This is also the reason why CBT for SBCC-C in Scenario 4 deviates more from the goal. In this scenario, new vehicles start at one end and drive normally approaching to the traffic jam. During their approach to the traffic jam they use high power since they do not discover too many neighbors in their surroundings. In fact, the number of vehicles trapped in the traffic jam is large, but since their local density is high, they have already reduced their power and so approaching cars are not aware of them until they are close enough. In summary, the local density of cars measured by the approaching cars is much lower than the measured by the cars in the traffic jam. This is precisely the situation for which application of *edge correction* is intended, where we can expect noticeable differences in local densities, and more importantly, sustained in time. SUMO reports at the traffic jam a density of $\rho_1 = 0.21$ whereas in the rest of the road the density is around $\rho_2 = 0.09$. Since it is a dynamic scenario, the performance degradation estimates of Sect. IV-B cannot be applied directly. In Fig. 8 we have plotted the average CBT for every vehicle in scenarios 1 and 3. The traffic jam scenario shown in Fig. 8(b) reflects an extra load around 0.05 to 0.10 (in CBT), which is close to the estimated l_{em} for those densities. On the contrary, when *edge correction* is used the extra load decreases to around 0.05 which is the intended goal with $\alpha_s = 0.15$. In addition, as intended, it makes a fraction of nodes on the edge of the traffic jam keep a higher power, which creates an extended safety range for vehicles approaching. As the traffic jam queue increases, these nodes reduce their power according to the local density and the newly arrived keep the higher power at the edge. However, applying *edge correction* in the normal traffic scenarios results is a global reduction of the CBT. The reason is that in a normal situation the local densities are not homogeneous and vehicles tend to move in separated clusters. In that situation, the fraction of beacons from ahead and behind, f_a and f_b tend to be more asymmetric, which makes nodes apply *edge correction* and force an artificial reduction of the transmit power of nodes at the center of clusters. Whether this extra reduction is beneficial or not depends on the intended goal, if a reduction of CBT to 0.6 is acceptable it results in a slight increment of the effective beaconing rate. A trade-off solution, since *edge correction* achieves its goals in the intended scenario, is to apply it dynamically. For instance, it can be turned on only when vehicles actually detect a traffic jam (slow speed and high density of surrounding vehicles). In any case, a more thorough study of the possibilities is left as future work.

Regarding powers, results of Fig. 7(c) have to be adequately interpreted, because they show time-averages of quite different values, as reflected by the confidence intervals. Since vehicles start using high powers, and then gradually reduce it according to the local density, it is more revealing to look at the time

Algorithm	$\hat{\rho}$	$\hat{\beta}$	$\hat{m}$
Scenario 1. A5 highway with normal traffic and $\beta = 2.5 \quad m = 1$			
SBCC-C	0.06 ± 0.01	2.56 ± 0.00	1.36 ± 0.01
SBCC-N	0.08 ± 0.01	2.56 ± 0.00	1.38 ± 0.01
Scenario 2. A5 highway with normal traffic and $\beta = 2.5 \quad m = 3$			
SBCC-C	0.06 ± 0.01	2.52 ± 0.00	3.49 ± 0.01
SBCC-N	0.06 ± 0.01	2.52 ± 0.00	3.48 ± 0.01
Scenario 3. A5 highway with traffic jam and $\beta = 2.5 \quad m = 1$			
SBCC-C	0.10 ± 0.03	2.58 ± 0.00	1.29 ± 0.02
SBCC-N	0.11 ± 0.03	2.57 ± 0.01	1.29 ± 0.02
Scenario 4. A5 highway with traffic jam and $\beta = 2.5 \quad m = 3$			
SBCC-C	0.10 ± 0.03	2.53 ± 0.00	3.36 ± 0.08
SBCC-N	0.09 ± 0.02	2.53 ± 0.00	3.40 ± 0.02

TABLE V
ESTIMATES FOR DYNAMIC SCENARIOS

evolution. For instance, for SBCC-C in Scenario 3, we have collected window averages of transmit power every 25 s. In that case we obtain averages for the first batches of 785 mW, 204 mW, 28.1 mW, 18.3 mW, 21.1 mW. The global average is raised due to the high difference between the first samples and subsequent ones. We show only the global averages in 7(c) to illustrate the global trend between different algorithms.

SPAV results are again close to those of SBCC-N though it tends to be more conservative and reduces the power more and for a longer timer. Not using TPC again results in the channel being almost completely occupied by beaconing activity and unacceptable channel access time higher. Finally, results show again that the effective beaconing rate, when power control is used, is mainly determined by the fading conditions and hidden node collisions. When no TPC is used it worsens due to additional in-range collisions and channel congestion.

Table V shows that estimates are correct also for dynamic scenarios. Regarding density, SUMO reports an average density of 0.065 vehicles/m for Scenarios 1 and 2 and 0.09 for Scenarios 3 and 4, which coincides with the values measured by vehicles. But this is a globally averaged value. In the traffic jam scenarios the local density at the traffic jam is much higher, rising up to 0.21 vehicles/m. The difference in the local densities along the path also accounts for the seemingly high average power shown in Fig. 7(c): since the density is around 0.09 one would expect power to be in the order of those shown in Fig. 5(c) in previous section. But vehicles use high power at the beginning of the journey and so the average is raised and the variance is higher.

Overall, the performance evaluation results discussed in this section confirm that our proposals SBCC-C and SBCC-N provide an effective technique to control channel congestion due to beaconing activity in realistic scenarios with non-homogeneous traffic densities and dynamic environments.

VII. CONCLUSIONS

In this paper we propose and discuss a novel statistical approach to TPC for beaconing congestion control in vehicular networks, called Statistical Beaconing Congestion Control (SBCC). With this algorithm each vehicle computes locally the maximum power needed to comply with a given maximum beacon load as a function of the channel parameters, average vehicle density and neighbor transmit power. We derive a final expression of the algorithm as a linear proportional controller and provide two variants, SBCC-C and SBCC-N, depending on how the vehicle density is estimated. Unlike previous proposals, SBCC adds little overhead to the communications. Our results show that SBCC is able to effectively control beaconing congestion and improve other performance metrics in dynamic scenarios with non-homogeneous networks.

Edge effects and differences of densities sustained in time lower the performance of SBCC. We propose edge correction, a mechanism to overcome it while keeping an extended range for nodes at the edge of the cluster, which is useful as a warning range for vehicles approaching a traffic jam. Additionally, we derive an approximate expression for the estimated communication range under interference, r_E, and what we call the interference range, r_I. The latter in fact provides the average fraction of packets lost due to hidden node collisions. Hence, it is necessary to correctly estimate either the effective beaconing rate or the actual CBT generated by a number of vehicles, among other metrics. It can be also used to compensate the error in the estimation of the vehicle density and as a fast recovery mechanism when channel load is high.

We have shown how, with SBCC, TPC fulfills its goal and makes channel load and effective beaconing rate independent of vehicle density. In that case, the reliability of beacon reception is basically determined by hidden node collisions and fading, and can be estimated by r_I. So we plan to leverage on it to evaluate combinations of beaconing rate and transmit power that are able to meet the requirements of different applications. Moreover, the estimated communication range under interference can be useful in the design of emergency or multihop warning delivery message applications, where the delay and reliability of the service is also determined by hidden node collisions and connectivity.

Indeed, the next natural step is to build integrated, application-based awareness control schemes. The challenge is how to integrate seamlessly them with congestion control. SBCC is a proactive algorithm, which uses estimates that reflect the average propagation conditions in order to limit congestion for all nodes. Awareness control implies adapting

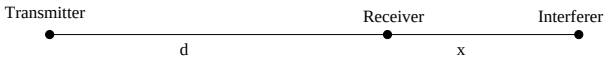

Fig. 9. Interference model

the power or rate of a selected subset of nodes to comply with the requirements of a particular application. It is necessary to evaluate the influence of specific modifications of a subset of nodes on the rest of them and the stability of the controls. Hence, our plan is to develop awareness-control schemes on top of SBCC, taking into account stability constraints. Stability is indeed important even without further developments, so as a first next step we plan to analyze the stability of SBCC.

As a future work we also intend to evaluate the performance of SBCC when the channel is not correctly modeled by a Nakagami-m model or nodes experience different fading conditions.

APPENDIX
COMPUTATION OF INTERFERENCE RANGE

When the load in the channel is high, a fraction of the vehicles in carrier sense range r_{CS} will not receive the messages because of hidden nodes transmissions. To derive it, let us consider a transmitter located at the origin $X_T = 0$, a receiver located at a distance d along the x axis and one interferer (hidden node) located at a distance $d + x$ from the transmitter. As a worst case approach we only consider the stronger interferer, as shown in Fig. 9.

We assume the system model described in Sect. III-A. Neglecting noise and interference from other nodes, which is reasonable as discussed in Sect. III-C, a message is received correctly at d if the ratio of the received power from the transmitter to the received power from the interferer is above a given threshold T. Let be $\mathbf{F_T}$ and $\mathbf{F_H}$ the virtual power emitted from transmitter and interferer (hidden node) respectively, then a packet is correctly received if $\frac{\mathbf{F_T}}{Ad^\beta} \geq T\frac{\mathbf{F_H}}{Ax^\beta}$.

Let us consider a given transmitter power p_T and interferer power p_H. If we consider a Nakagami-m fading channel let $I(F_T, d, x)$ be the probability that a packet is interfered conditioned on F_T, d and x:

$$I(F_T, d, x) = P(\mathbf{F_H} > \frac{F_T x^\beta}{Td^\beta}) = \frac{\Gamma(m, \frac{F_T m}{Tp_H}(\frac{x}{d})^\beta)}{\Gamma(m)} \quad (15)$$

Now we uncondition on F_T, but taking into account that: (1) receiver must be in transmission range, that is, $F_T \geq SAd^\beta$; and (2), hidden node cannot be in transmission range, that is, $F_T < SA(x + d)^\beta$:

$$I(d, x) = \int_{SAd^\beta}^{SA(d+x)^\beta} \frac{\Gamma(m, y\frac{m}{Tp_H}(\frac{x}{d})^\beta)}{\Gamma(m)} f(y)\mathrm{d}y \quad (16)$$

In order to obtain a tractable expression for the interference range, we have to further assume that the m parameter is an integer. In that case, the gamma distribution becomes an Erlang distribution, whose distribution function is $F(x) = 1 - \sum_{i=0}^{m-1} e^{-\mu x}\frac{(\mu x)^i}{i!}$ and probability density function is $f(x) = \frac{\mu^m x^{m-1}}{(m-1)!}e^{-\mu x}$. To simplify notation let $B = SAd^\beta$, $C = SA(d + x)^\beta$ and $K = \frac{m}{Tp_H}(\frac{x}{d})^\beta$. Let us also recall that $\mu_H = \frac{m}{p_H}$ and $\mu_T = \frac{m}{p_T}$. Then, substituting Gamma by an Erlang distribution and its pdf, the probability of interference becomes

$$\begin{aligned} I_E(d, x) &= \int_B^C \left(\sum_{i=0}^{m-1} e^{-Ky}\frac{(Ky)^i}{i!}\right)\frac{\mu_T^m y^{m-1}}{(m-1)!}e^{-\mu_T y}\mathrm{d}y = \\ &= \frac{\mu_T^m}{(m-1)!}\left(\sum_{i=0}^{m-1}\int_B^C \frac{e^{-(K+\mu_T)y}}{i!}K^i y^{i+m-1}\mathrm{d}y\right) = \\ &= \frac{\mu_T^m}{(m-1)!}\sum_{i=0}^{m-1}\frac{K^i}{i!(\mu_T + K)^{m+i}}\cdot \\ &\cdot \Big(\Gamma(m+i, B(\mu_T + K)) - \Gamma(m+i, C(\mu_T + K))\Big) \end{aligned} \quad (17)$$

Previous equation gives the probability that a packet at some point (receiver location) is not received due to interference as a function of the distance to the transmitter and hidden node. To get an average over the set of all locations we apply Robbin's formula [32], and integrate $I_E(d, x)$ over all the set of points:

$$r_I = \int_0^\infty \int_0^\infty I_E(d, x)\mathrm{d}x\mathrm{d}d \quad (18)$$

To compute the integral above we change the order of integration and introduce an auxiliary variable α as $x = d(\alpha - 1)$. Then α varies from 1, when the distance from the hidden node to the receiver is 0, to $+\infty$, and eq. (18) becomes

$$\begin{aligned} r_I = &\frac{\mu_T^m}{(m-1)!}\sum_{i=0}^{m-1}\int_1^\infty\int_0^\infty \frac{(\frac{\mu_H}{T}(\alpha-1)^\beta)^i}{i!(\mu_T + \frac{\mu_H}{T}(\alpha-1)^\beta)^{m+i}} \\ &\Big[\Gamma(m+i, SAd^\beta(\mu_T + \frac{\mu_H}{T}(\alpha-1)^\beta)) \quad - \\ &- \quad \Gamma(m+i, SA(d\alpha)^\beta(\mu_T + \frac{\mu_H}{T}(\alpha-1)^\beta))\Big]\mathrm{d}d\mathrm{d}\alpha = \\ &= \frac{\mu_T^m}{(m-1)!}\sum_{i=0}^{m-1}(I_1 - I_2) \end{aligned} \quad (19)$$

To simplify notation let us define

$$G(\alpha, m, i) = \frac{(\frac{\mu_H}{T}(\alpha-1)^\beta)^i}{i!(\mu_T + \frac{\mu_H}{T}(\alpha-1)^\beta)^{m+i}}$$
$$R = SA(\mu_T + \frac{\mu_H}{T}(\alpha-1)^\beta)$$

We compute the first integral as

$$I_1 = \int_1^\infty\int_0^\infty G(\alpha, m, i)\left(\int_{Rd^\beta}^\infty t^{m+i-1}e^{-t}\mathrm{d}t\right)\mathrm{d}d\mathrm{d}\alpha \quad (20)$$

Then, changing the order of the inner iterated integral we get

$$\begin{aligned} I_1 &= \int_1^\infty G(\alpha,m,i)\int_0^\infty t^{m+i-1}e^{-t}\int_0^{(\frac{t}{R})^{\frac{1}{\beta}}} \mathrm{d}d\mathrm{d}t\mathrm{d}\alpha = \\ &= \int_1^\infty G(\alpha,m,i)\frac{1}{R^{\frac{1}{\beta}}}\int_0^\infty t^{m+i-1+\frac{1}{\beta}}e^{-t}\mathrm{d}t\mathrm{d}\alpha = \\ &= \int_1^\infty G(\alpha,m,i)\frac{1}{R^{\frac{1}{\beta}}}\Gamma(m+i+\frac{1}{\beta})\mathrm{d}\alpha \end{aligned} \tag{21}$$

And similarly

$$I_2 = \int_1^\infty G(\alpha,m,i)\frac{1}{R^{\frac{1}{\beta}}}\frac{\Gamma(m+i+\frac{1}{\beta})}{\alpha}\mathrm{d}\alpha \tag{22}$$

So finally, the interference range becomes

$$\begin{aligned} r_I = \frac{\mu_T^m}{(m-1)!}\sum_{i=0}^{m-1}\frac{1}{i!}\Bigg(\int_1^\infty \frac{(\frac{\mu_H}{T}(\alpha-1)^\beta)^i}{(\mu_T+\frac{\mu_H}{T}(\alpha-1)^\beta)^{m+i}} \\ \frac{\Gamma(m+i+\frac{1}{\beta})}{(SA\mu_T)^{\frac{1}{\beta}}(1+\frac{\mu_H}{T\mu_T}(\alpha-1)^\beta)^{\frac{1}{\beta}}}\frac{\alpha-1}{\alpha}\mathrm{d}\alpha\Bigg) \end{aligned} \tag{23}$$

And to express it as a product of the transmission range we use the fact that $\Gamma(m+n)=\Gamma(m)(m)_n$, where $(m)_n$ is a *Pochhammer symbol* or *rising factorial*:

$$\begin{aligned} r_I = r_{CS}\frac{\mu_T^m}{(m-1)!}\sum_{i=0}^{m-1}\frac{1}{i!}\Bigg(\int_1^\infty \frac{(\frac{\mu_H}{T}(\alpha-1)^\beta)^i}{(\mu_T+\frac{\mu_H}{T}(\alpha-1)^\beta)^{m+i}} \\ \frac{(m+\frac{1}{\beta})_i}{(1+\frac{\mu_H}{T\mu_T}(\alpha-1)^\beta)^{\frac{1}{\beta}}}\frac{\alpha-1}{\alpha}\mathrm{d}\alpha\Bigg) \end{aligned} \tag{24}$$

Let us note that when $m=1$ (Rayleigh fading) this expression simplifies to

$$r_I = r_{CS}\int_1^\infty \frac{\alpha-1}{\alpha\left(1+\frac{p_T(\alpha-1)^\beta}{p_H T}\right)^{\frac{\beta+1}{\beta}}}\mathrm{d}\alpha \tag{25}$$

REFERENCES

[1] H. Hartenstein and K. P. Laberteaux, *VANET. Vehicular Applications and Inter-Networking Technologies*, Wiley, 2010.

[2] *Intelligent Transport Systems (ITS); Access layer specification for Intelligent Transport Systems operating in the 5 GHz frequency band*, v1.2.1, ETSI EN 302 663, May 2013.

[3] *IEEE Standard for Information technology–Telecommunications and information exchange between systems Local and metropolitan area networks–Specific requirements Part 11: Wireless LAN Medium Access Control (MAC) and Physical Layer (PHY) Specifications*, IEEE Std 802.11-2012, March 2012.

[4] G. Karagiannis, O. Altintas, E. Ekici, G. Heijenk, B. Jarupan, K. Lin, and T. Weil, "Vehicular Networking: A Survey and Tutorial on Requirements, Architectures, Challenges, Standards and Solutions," *IEEE Communications Surveys & Tutorials*, vol. 13, no. 4, pp. 584-616, 2011.

[5] *Intelligent Transportation Systems (ITS); Vehicular Communications; Basic Set of Applications; Part 2: Specification of Cooperative Awareness Basic Service*, ETSI EN 302 637-2, v1.3.0, April 2013.

[6] C.-ling Huang, Y. P. Fallah, R. Sengupta, and H. Krishnan, "Adaptive Intervehicle Communication Control for Cooperative Safety Systems," *IEEE Network*, vol. 24, pp. 6-13, 2010.

[7] M. Sepulcre, J. Gozalvez, and H. Hartenstein, "Application-Based Congestion Control Policy for the Communication Channel in VANETs," *IEEE Communications Letters*, vol. 14, no. 10, pp. 951-953, 2010.

[8] L. Cheng, B. E. Henty, D. D. Stancil, F. Bai, and P. Mudalige, "Mobile Vehicle-to-Vehicle Narrow-Band Channel Measurement and Characterization of the 5.9 GHz Dedicated Short Range Communication (DSRC) Frequency Band," *IEEE Journal on Selected Areas in Communications*, vol. 25, no. 8, pp. 1501-1516, 2007.

[9] M. Torrent-Moreno, J. Mittag, P. Santi, and H. Hartenstein, "Vehicle-to-vehicle Communication: Fair Transmit Power Control for Safety-Critical Information", *IEEE Transactions on Vehicular Technology*, vol.58, no. 7, pp. 3684–3703, Sept. 2009.

[10] K. Ogata, *Discrete-time Control Systems*, Prentice-Hall, 2nd edition, 1995.

[11] *Intelligent Transport Systems (ITS); Decentralized Congestion Control Mechanisms for Intelligent Transport Systems operating in the 5 GHz range; Access Layer part*, ETSI TS 102 687, 2011.

[12] *Highway capacity manual-HCM 2000*. Transportation Research Board, National Research Council, 2000.

[13] R. Schmidt, T. Leinmuller, E. Schoch, F. Kargl, and G. Schafer, "Exploration of Adaptive Beaconing for Efficient Intervehicle Safety Communication," *IEEE Network*, vol. 24, no. 1, pp. 14-19, Jan. 2010.

[14] J. B. Kenney, G. Bansal, and C. E. Rohrs, "LIMERIC: a Linear Message Rate Control Algorithm for Vehicular DSRC Systems," *Proceedings of the eighth ACM international workshop on Vehicular Inter-networking (VANET 2011)*, pp. 21-30, 2011.

[15] T. Tielert, D. Jiang, Q. Chen, L. Delgrossi, and H. Hartenstein, "Design Methodology and Evaluation of Rate Adaptation Based Congestion Control for Vehicle Safety Communications," *IEEE Vehicular Networking Conference (VNC 2011)*, pp. 116-123, 2011.

[16] J. Mittag, F. Schmidt-Eisenlohr, M. Killat, J. Harri, and H. Hartenstein, "Analysis and Design of Effective and Low-Overhead Transmission Power Control for VANETs", *Proceedings of the fifth ACM international workshop on Vehicular Inter-networking (VANET 2008)*, 2008.

[17] M. Artimy, "Local Density Estimation and Dynamic Transmission-Range Assignment in Vehicular Ad Hoc Networks", *IEEE Transactions on Intelligent Transportation Systems*, vol. 8, no. 3, September 2007.

[18] M. Sepulcre, J. Mittag, P. Santi, H. Hartenstein, and J. Gozalvez, "Congestion and Awareness Control in Cooperative Vehicular Systems," *Proceedings of the IEEE*, vol. 99, no. 7, pp. 1260-1279, 2011.

[19] J. Gozalvez and M. Sepulcre, "Opportunistic Technique for Efficient Wireless Vehicular Communications," *IEEE Vehicular Technology Magazine*, vol. 2, no. 4, pp. 33-39, 2007.

[20] V. G. Douros and G. C. Polyzos, "Review of some Fundamental Approaches for Power Control in Wireless Networks," *Computer Communications*, vol. 34, no. 13, pp. 1580-1592, Aug. 2011.

[21] P. Cardieri, "Modeling Interference in Wireless Ad Hoc Networks," *IEEE Communications Surveys & Tutorials*, vol. 12, no. 4, pp. 551-572, 2010.

[22] F. Baccelli and B. Błaszczyszyn, "Stochastic Geometry and Wireless Networks Volume 1: THEORY", *Foundations and Trends in Networking* vol. 3: No 3-4, pp 249-449, 2009.

[23] F. Baccelli and B. Błaszczyszyn, "Stochastic Geometry and Wireless Networks Volume 2: APPLICATIONS", *Foundations and Trends in Networking* vol. 4: No 1-2, pp 1-312, 2009 .

[24] S. Srinivasa and M. Haenggi, "Path Loss Exponent Estimation in Large Wireless Networks," *Information Theory and Applications Workshop*, pp. 124-129, 2009.

[25] Q. Zhang, "A Note on the Estimation of Nakagami-m Fading Parameter," *IEEE Communications Letters*, vol. 6, no. 6, pp. 237-238, 2002.

[26] T. Y. Hwang and P. H. Huang, "On New Moment Estimation of Parameters of the Gamma Distribution Using its Characterization," *Annals of the Institute of Statistical Mathematics*, vol. 54, no. 4, pp. 840-847, 2002.
[27] Qi Chen, D. Jiang, T. Tielert, and L. Delgrossi, "Mathematical Modeling of Channel Load in Vehicle Safety Communications ," *Vehicular Technology Conference (VTC Fall)*, p. 1-5, 2011.
[28] OMNeT++ simulation library. [Online]. Available at http://www.omnetpp.org
[29] C. Sommer, R. German and F. Dressler, "Bidirectionally Coupled Network and Road Traffic Simulation for Improved IVC Analysis," *IEEE Transactions on Mobile Computing* , vol. 10, no. 1, pp. 3-15, 2011.
[30] M. Behrisch, L. Bieker, J. Erdmann, and D. Krajzewicz, "SUMO - Simulation of Urban MObility: An Overview," *The Third International Conference on Advances in System Simulation (SIMUL 2011)*, 2011.
[31] Open Street Map. [Online]. Available at http://www.openstreemap.org
[32] Hung T. Nguyen, *An Introduction to Random Sets*, CRC Press, 2006.

Andreas Festag received a diploma degree (1996) and Ph.D. (2003) in Electrical Engineering from the Technical University Berlin. As researcher, he worked at Technical University Berlin, Heinrich-Hertz-Institute (HHI) in Berlin and NEC Laboratories in Heidelberg, where he lastly had the position of a Chief Researcher. He joined the Technical University Dresden, Vodafone Chair Mobile Communications Systems, in 2013 as a research group leader. Andreas was involved in various research projects for wireless and mobile communication networks and published more than 50 papers in journals, conference proceedings and workshops. His research is concerned with architecture, design and performance evaluation of wireless and mobile communication systems and protocols, in the past years with a focus on vehicular communication and Intelligent Transportation Systems (ITS). He actively contributes to the CAR-2-CAR Communication Consortium and to ITS standardization in ETSI Technical Committee ITS, where he is chairman of the working group Networking & Transport.

Esteban Egea-Lopez received the Telecommunications Engineering degree in 2000, from the Universidad Politécnica de Valencia (UPV), Valencia, Spain, the Master Degree in Electronics in 2001, from the University of Gavle, Sweden, and Ph.D. in Telecommunications in 2006 from the Universidad Politécnica de Cartagena (UPCT), Cartagena, Spain. Since 2001, he is an associate professor of the Department of Information Technologies and Communications at UPCT. His research interest is focused on wireless networks, including RFID and vehicular networks.

Juan J. Alcaraz obtained his engineering degree from the Universidad Politécnica de Valencia (UPV), Valencia, Spain in 1999. After working for several telecommunication companies he joined the Universidad Politécnica de Cartagena (UPCT), Cartagena, Spain in 2004, where he obtained his Ph.D. in 2007 and currently works as associate professor. His research interests lie in the field of wireless communications, including cognitive radio, vehicular networks and radio frequency identification systems.

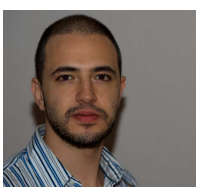

Javier Vales-Alonso is an Associate Professor with the Department of Information Technologies and Communications, Universidad Politécnica de Cartagena (UPCT), Spain. His main research interests lie in wireless communication areas, mainly in the fields of cellular networks, wireless sensor networks, cognitive radio, vehicular networks, and radio identification. He has been involved in several Spanish national research projects related to development of ambient intelligence applications.

Joan Garcia-Haro received the M.Sc and Ph.D degrees in telecommunication engineering from the Universitat Politecnica de Catalunya, Barcelona, Spain, in 1989 and 1995, respectively. He is currently a Professor with the Universidad Politécnica de Cartagena (UPCT). He is author or co-author of more than 70 journal papers mainly in the fields of switching, wireless networking and performance evaluation. From April 2002 to December 2004 he served as Editor-in-Chief of the IEEE Global Communications Newsletter, included in the IEEE Communications Magazine. He was Technical Editor of the same magazine from March 2001 to December 2011. He also holds an Honorable Mention for the IEEE Communications Society Best Tutorial paper Award (1995). He has been a visiting scholar at Queen's University at Kingston, Canada (1991-1992) and at Cornell University, Ithaca, USA (2010-2011).